A Two-Level Model of a Thermally Forced Ocean Basin

M. K. DAVEY

Department of Applied Mathematics and Theoretical Physics, University of Cambridge, Cambridge CB39EW England

(Manuscript received 29 April 1982, in final form 7 October 1982)

ABSTRACT

Some simple solutions (mostly analytic) are presented for the large-scale baroclinic response to thermal forcing on a mid-latitude beta-plane. Surface heat flux is parameterized as $(T_A - T_T)/\tau$, with atmospheric temperature T_A prescribed as a function of latitude, varying ocean surface temperature T_T, and equilibration time τ. For long times (decades) benthic forcing is included, using a similar representation. The model allows horizontal density variations at each level.

When there are no meridional boundaries there is only a local response to the forcing. A geostrophic baroclinic zonal flow is driven by the north–south temperature gradient, but it has no associated advection or divergence effects. This picture is greatly changed when east and/or west coasts are added. Kelvin waves pass information rapidly (about 200 km day^{-1}) along coasts, and Rossby waves travel slowly offshore, most effectively from the east with speed $c \approx 1$ km day^{-1}. For spin-up problems (e.g., the response to a change in forcing) the long Rossby waves decay away from the eastern boundary on a scale $c\tau$. With T_A decreasing poleward this creates a broad, relatively warm eastern region with weak downwelling. A steady state requires weaker vertical motion to balance benthic forcing and a corresponding larger decay scale. The narrow western boundary layer is relatively cold on average, with upwelling. (This two-level model does not adequately describe western boundary dynamics, however.)

1. Introduction

The oceans are driven by both surface wind stress and density changes. Many large-scale features of the observed currents have been explained using simple wind-driven models with one or more layers of constant density—see for example Stommel's (1948) explanation of western intensification, or the world ocean model constructed by Veronis (1973). To explain density distributions, however, some thermodynamics must be included.

A thermohaline circulation can be simulated in multi-layer models by adding a source–sink flow, with mass flux from one layer to another. [Veronis (1976) used this technique, with uniform upwelling through the thermocline balancing sinking at high latitudes, in extensions to his wind-driven theory.] However, this approach does not allow density variations within each layer.

More detailed density distributions can be simulated using the steady thermocline equations, driven by surface temperature (or heat flux) and vertical velocity (Ekman pumping). These nonlinear equations have interesting exact similarity solutions (see Welander, 1971, for example). Unfortunately such solutions are limited in application by their special nature. Barcilon (1971) presents a simpler linear theory that allows western as well as eastern boundaries, but geostrophic restrictions still require constant longshore densities.

Another approach is to numerically solve more general equations. Bryan and Cox (1967) investigated the response to thermal forcing by this method, comparing several cases with and without wind stress, using a six level model. [They also used a similarity solution by Robinson and Welander (1963) as a test case.] A wide range of physics can be incorporated, and many such models of increasing resolution and complexity have been developed in recent years, ranging from process models to detailed ocean/atmosphere simulations.

There seems to be a need for further simple large-scale models that have varying density. This paper describes a model that has independent density variations at each of two levels. It is driven by a surface heat flux, proportional to the difference between a prescribed effective atmospheric temperature T_A and the sea surface temperature T_T. To avoid difficulties associated with different mixing for heating and cooling, only cooling ($T_A < T_T$) is considered. For large time scales (several years) benthic forcing is needed. Rather than prescribe a vertical velocity, the deep water is forced toward some equilibrium density on a long time scale.

Linear longshore geostrophic momentum and nonlinear heat equations for a mid-latitude β-plane are used. For simplicity only thermally driven density changes are considered. [With regard to benthic processes, temperature should be regarded as an apparent temperature, as defined by Fofonoff (1962).] In the

absence of surface or bottom stress the flow is purely baroclinic. Further details of the basic equations and associated assumptions are given in the next section.

In Section 3 the short-term response to switching on a heat flux is described in terms of linear f-plane coastal Kelvin waves. These waves rapidly pass information from one latitude to another. For longer times, Rossby waves transmit information away from the coasts. This effect is investigated in Section 4 for forcing, independent of time. Feedback effects due to the dependence of heat flux on ocean temperature become important, and in Section 5 we find that the long Rossby waves that control the eastern region then decay westward. The decay scale is the product of the longwave speed and the time scale for local adjustment to the forcing.

Steady linear and nonlinear models, with west as well as east coasts, are investigated in Section 6 with various forms of longshore velocity damping. The limited vertical resolution causes difficulties in the narrow western boundary layer, where unreasonably large static stability is generated.

The mathematical strategy used is to reduce the problem to ordinary differential equations at each latitude. In most cases these can be solved analytically, and where numerical methods are needed (Section 6), high-resolution solutions can be readily obtained.

2. Basic equations, forces, and scales

The two-level geometry is shown in Fig. 1a. The vertical finite-difference approximation that is used allows independent horizontal density variations at each level, as outlined in Appendix A. It is analogous to the two-level atmospheric model introduced by Lorenz (1960). [See also Bryan (1969) for a description of a multi-level ocean model, and Killworth (1974) for a two-layer Antarctic shelf sea model with varying density.]

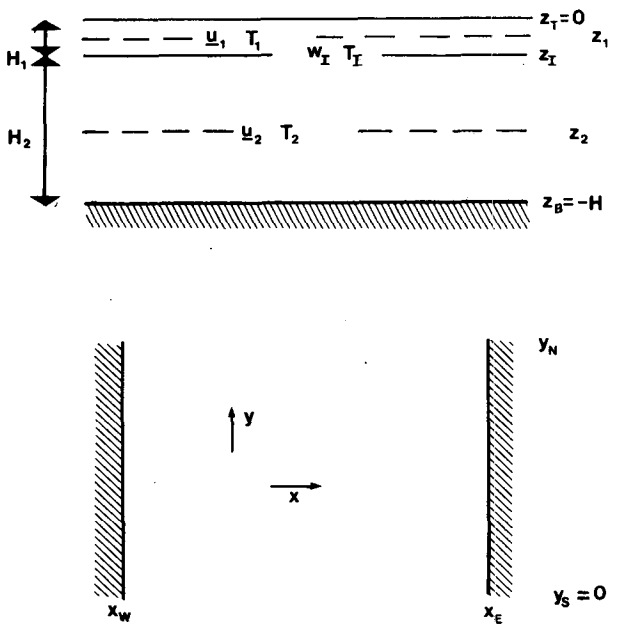

FIG. 1. (a) Two two-level geometry: vertical section showing depths and main variables. (b) Horizontal plan of the basin with east and west coasts.

Density ρ may change as temperature or salinity varies. For simplicity only variations in temperature T will be considered, so

$$\rho = \rho_c[1 - \alpha(T - T_c)], \tag{2.1}$$

where ρ_c and T_c are reference scales, and $\alpha = 10^{-4}$ °C^{-1} is the thermal expansion coefficient. The basic dynamic variables are the temperatures $T_j(x, t)$ and velocities $u_j(x, t)$ at levels $j = 1, 2$, where

$$\mathbf{x} = (x, y), \quad \mathbf{u} = (u, v)$$

are horizontal vectors. The levels are at depths

$$z_1 = -H_1/2, \quad z_2 = -H_1 - H_2/2,$$

the sea surface being at $z_T = 0$ and flat bottom at $z_B = -(H_1 + H_2) = -H$. To make the best use of the limited vertical resolution the variables at level j should be representative of averages over depth H_j. (This also reflects the close relation of level and depth-averaged models.) We will use

$$H_1 = 400 \text{ m}, \quad H_2 = 3600 \text{ m}$$

to represent the basic baroclinic structure of the ocean.

With no surface wind stress or bottom friction to drive Ekman pumping the flow in this model generally has no barotropic component, so

$$H_1\mathbf{u}_1 + H_2\mathbf{u}_2 = \mathbf{0}. \tag{2.2a}$$

In terms of the difference $\mathbf{U} = \mathbf{u}_1 - \mathbf{u}_2$, we have

$$\mathbf{u}_1 = (1 - \delta)\mathbf{U}, \tag{2.2b}$$

$$\mathbf{u}_2 = -\delta\mathbf{U}, \tag{2.2c}$$

where $\delta = H_1/(H_1 + H_2)$. For the depths given above, $\delta = 0.1$.

a. Equations

In flux form the temperature equation at the two levels gives

$$T_{1t} + \nabla\cdot(\mathbf{u}_1T_1) - w_IT_I/H_1 = F_1, \tag{2.3a}$$

$$T_{2t} + \nabla\cdot(\mathbf{u}_2T_2) + w_IT_I/H_2 = F_2, \tag{2.3b}$$

where F_j represents thermal forcing. (Subscripts t, x, y indicate partial derivatives.) The temperature T_I at the intermediate depth $z_I = -H_1$ is related to T_1 and T_2 by

$$T_I = \tfrac{1}{2}(T_1 + T_2).$$

(Other choices are possible—see Appendix A for de-

tails.) The vertical velocity w_I at the depth z_I is related to the divergence $\nabla \cdot \mathbf{U}$ by

$$w_I = (1 - \delta)\delta H \nabla \cdot \mathbf{U}.$$

From (2.3) we obtain, for future reference,

$$(H_1T_1 - H_2T_2)_t + 2\delta(1 - \delta)H\mathbf{U} \cdot \nabla T_I = H_1F_1 - H_2F_2. \quad (2.4)$$

Linear momentum equations will be used because currents generated by large-scale thermal forcing are generally weak. Only east and west coasts will be considered, as indicated in Fig. 1b. Away from these boundaries geostrophic balance is anticipated. Assuming longshore geostrophy gives

$$fV = \phi_x, \quad (2.5a)$$

where $f = f_0 + \beta y$ is the Coriolis parameter for a midlatitude β-plane, and

$$\phi = \tfrac{1}{2}H\alpha g(T_I - T_c) \quad (2.6)$$

is a potential function. Ageostrophic effects are retained in the longshore velocity equation

$$V_t + fU = -\phi_y - \mathcal{D}. \quad (2.5b)$$

The term V_t allows propagation of coastal Kelvin waves, and some function $\mathcal{D}$ is included to simulate damping of these waves by effects such as nonlinearity, shelf interaction and dissipation. Various forms for $\mathcal{D}$ can be postulated, and we choose the simplest (as used by Stommel 1948):

$$\mathcal{D} = KV, \quad (2.7)$$

where K is a constant damping rate. (Other possibilities are mentioned in Section 6.) For a steady state $\mathcal{D}$ breaks the geostrophy that would otherwise require T_I constant along the coast, where $U = 0$. (An important aspect of this model is that the geostrophic assumption of constant longshore T_I can be tested.)

For later reference we note that advection and divergence can be written in terms of V as

$$\tfrac{1}{2}H\alpha g\mathbf{U} \cdot \nabla T_I = \mathbf{U} \cdot \nabla \phi = -V\mathcal{D} - VV_t, \quad (2.8a)$$

$$f\nabla \cdot \mathbf{U} = -\beta V - \mathcal{D}_x - V_{xt}. \quad (2.8b)$$

Because currents are driven by gradients of T_I it is mathematically convenient to rewrite the temperature equations (2.3) in terms of T_I, and the difference

$$S = \tfrac{1}{2}(T_1 - T_2)$$

which is a measure of static stability. Reduced gravity g' is related to S by

$$g' = \tfrac{1}{4}\alpha g S.$$

It is also convenient to write

$$\left.\begin{aligned} T_I = T &= \tfrac{1}{2}(T_1 + T_2) \\ F &= \tfrac{1}{2}(F_1 + F_2) \end{aligned}\right\}.$$

Then $T_1 = T + S$, $T_2 = T - S$, and (2.3) becomes

$$T_t + (1 - 2\delta)\mathbf{U} \cdot \nabla T + \tfrac{1}{2}\nabla \cdot (\mathbf{U}S) = F, \quad (2.9a)$$

$$S_t + \tfrac{1}{2}\mathbf{U} \cdot \nabla T + \tfrac{1}{2}(1 - 2\delta)\nabla \cdot (\mathbf{U}S) = \tfrac{1}{2}(F_1 - F_2). \quad (2.9b)$$

In the following sections equations linearized about the initial values $T_0 = 7°C$ and $S_0 = 5°C$ will often be used:

$$T_t + \tfrac{1}{2}S_0\nabla \cdot \mathbf{U} = F, \quad (2.10a)$$

$$S_t + \tfrac{1}{2}(1 - 2\delta)S_0\nabla \cdot \mathbf{U} = \tfrac{1}{2}(F_1 - F_2). \quad (2.10b)$$

Eliminating $\nabla \cdot \mathbf{U}$ from (2.10) gives the simpler equation

$$(H_1T_1 - H_2T_2)_t = H_1F_1 - H_2F_2, \quad (2.11)$$

which is the linearized version of (2.4).

In special cases, as described in following sections and Appendix A, the equations can be further simplified.

b. *Thermal forcing*

To introduce the thermal forcing, first consider an upward surface heat flux Q spread uniformly by convection over a mixing depth H_M. Temperature changes over this depth are driven by

$$F_M = -Q/H_M\rho_c c_W, \quad (2.12)$$

where specific heat $c_W = 4.2$ J g^{-1} °C^{-1}. For example, $Q = 100$ W m^{-2} and $H_M = 400$ m gives $F_M = 6 \times 10^{-8}$ °C s^{-1} = 2°C year^{-1}.

In practice Q depends on the ocean–atmosphere temperature difference. From a data analysis, Haney (1971) obtained the zonally-averaged climatological relation

$$Q = Q_G(T_T - T_A), \quad (2.13)$$

where T_T is the ocean surface temperature, T_A is an apparent atmospheric temperature, and the annual mean gradient is approximately

$$Q_G = 30 \text{ W m}^{-1} \text{ °C}^{-1}.$$

Where $T_A < T_T$ and the upper ocean is cooling and overturning it seems reasonable to simply associate T_1 with T_T directly, and to write the upper level forcing due to the atmosphere as

$$F_A = (T_A - T_1)/\tau. \quad (2.14)$$

In the absence of other effects, T_1 adjusts to T_A on a time scale

$$\tau = H_M\rho_c c_W/Q_G.$$

Using the figures above, this equilibration time is approximately 600 days.

In regions where $T_A > T_T$, however, we expect tem-

perature changes to be confined to shallow surface layers, with diffusion to lower levels. This diffusion is relatively slow. For example, White and Bernstein (1981) deduced a vertical propagation rate of 50 m year^{-1} for temperature anomalies in the central Pacific. Effectively there is small warming on a long time scale for level 1 and over depth H_1 in the two level model. Such forcing could be roughly simulated using (2.14) with reduced effective T_A and large τ.

More elaborate and more realistic relations between surface forcing and F_1 can be constructed [see e.g., Adamec *et al.* (1981) for a combined mixed-layer, multi-level model], but then numerical methods are needed to obtain results, and mechanisms are often unclear. The purpose of this paper is to keep the dynamics as simple as possible, and only surface forcing of the form (2.14) will be considered.

For very long time scales the model requires some input to maintain the lower level temperature. This is achieved in practice by dense water forming at high latitudes and slowly advecting and diffusing to lower latitudes. Again, specific simulation of this process is complicated, involving mechanisms beyond the scope of this study. When considering long time scales, we shall simply prescribe a benthic forcing

$$F_B = -(T_2 - T_B)/\mathcal{T} \tag{2.15}$$

with some time scale $\mathcal{T} \gg \tau$. [This method of forcing toward an equilibrium temperature is similar to that used by Sarmiento and Bryan (1982) in their robust diagnostic model.]

For all examples in later sections we will use the (idealized) effective atmospheric temperature

$$T_A(y) = \begin{cases} T_S, & y < y_S \\ T_S + \tfrac{1}{2}(T_N - T_S)[1 - \cos\pi(y - y_S)/1], & y_S < y < y_S + 1 \\ T_N, & y_S + 1 < y \end{cases} \tag{2.16}$$

with $l = 2000$ km, $T_S = 12°C$, $T_N = 8°C$. (Subscripts N, S, E, W will denote values at y_N, y_S, x_E, and x_W.) This temperature distribution is plotted in Fig. 2. A constant benthic equilibrium temperature $T_B = 2°C$ will be prescribed.

Only forcing of the form $F_1 = F_A$ and $F_2 = F_B$ will be considered in the sections to follow. Some calculations were also made with vertical temperature diffusion proportional to $T_1 - T_2$ included, but the effect was minor and those results will not be further discussed.

For initial value cases, the constant initial conditions

$$\left.\begin{aligned} T_{10} &= T_A(y_S) = 12°C \\ T_{20} &= T_B = 2°C \end{aligned}\right\} \tag{2.17}$$

will be applied at $t = 0$.

c. *Local response*

With no east or west coasts and forcing a function of latitude only the dynamics is purely local:

$$\begin{aligned} T_{1t} &= F_1, \\ T_{2t} &= F_2 \end{aligned} \tag{2.18}$$

giving

$$\left.\begin{aligned} T_1 &= T_{10}\exp(-t/\tau) + T_A[1 - \exp(-t/\tau)] \\ T_2 &= T_B \end{aligned}\right\}. \tag{2.19}$$

The ensuing north–south temperature gradient drives a baroclinic geostrophic current U_g through the 'thermal wind' relation

$$f\mathbf{k} \times \mathbf{U}_g = -\nabla\phi.$$

In the present no-coast case we have only zonal flow:

$$\left.\begin{aligned} fU &= -\tfrac{1}{2}H\alpha g T_{Ay}[1 - \exp(-t/\tau)] \\ V &= 0 \end{aligned}\right\}.$$

For the scales given earlier, the maximum U is about 0.03 m s^{-1} at $y = 900$ km, attained on time scale τ. For later comparison maps of T_1 and U at $t = 2000$ days (effectively steady) are given in Fig. 3. Note that U vanishes north of $y = 2000$ km, where constant T_A is prescribed by (2.16).

For this simple no-coast example divergence and advection effects do not appear. The addition of east and/or west coasts changes the picture dramatically. The constraint of no flow normal to the boundaries generates coastal Kelvin waves, as described in the next section, and the β-effect allows Rossby waves to spread the coastal anomalies offshore.

3. Linear f-plane Kelvin waves

The dynamics of Kelvin waves is well known, so this description is brief. On an f-plane ($f = f_0$), with longshore damping [(2.7)], the linear temperature equation (2.10a) gives

$$T_t - L^2(T_{xxt} + KT_{xx}) = F, \tag{3.1}$$

where $L = (g'H)^{1/2}/f$ is the Rossby radius. (This scale for geostrophic adjustment is approximately 30 km for the figures given in the previous section.)

The coastal boundary condition $U = 0$ requires

$$f_0 T_y + T_{xt} + KT_x = 0 \tag{3.2}$$

at x_E and x_W. (The geostrophic zonal flow associated

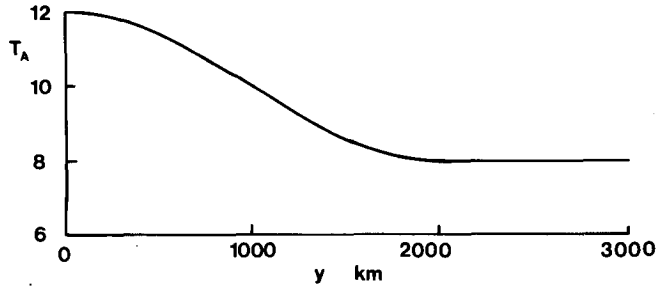

FIG. 2. The effective atmospheric temperature $T_A(y)$ used to force the upper level of the model.

with any longshore gradient of T must be balanced by ageostrophic terms.)

a. Spin-up with constant F (no feedback)

We first consider the response to forcing without feedback:

$$F_1 = (T_A - T_{10})/\tau$$

$$F_2 = (T_B - T_{20})/\tau = 0$$

gives

$$F = F_0 = (T_A - T_{10})/2\tau$$
$$= (T_A + T_B - 2T_0)/2\tau . \qquad (3.3)$$

Then (3.1) involves T alone, and can be readily solved using Laplace transforms. The solution is particularly simple when $K = 0$. Then at an east coast

$$T_E = T_0 + \int_0^t F_0(y - Ct')dt', \qquad (3.4)$$

where $C = fL = (g'H)^{1/2}$ is the Kelvin wave speed, typically about 200 km day^{-1}. The coastal response depends on information carried from distances up to Ct "upstream" by the Kelvin waves. The effect of the coast decays offshore with scale L, giving

$$T = T_L[1 - \exp(-X)] + T_E \exp(-X), \qquad (3.5)$$

where

$$X = (x_E - x)/L > 0,$$

and

$$T_L = T_0 + F_0 t$$

is the local (no coast) response.

With forcing by T_A that is decreasing poleward the east coast is warmer than the interior. Then the meridional flow

$$V = \tfrac{1}{2}H\alpha g(T_E - T_L)\exp(-X)/C \qquad (3.6)$$

is positive, poleward at the upper level and equatorward below. Further, with $w_I < 0$ there is downwelling in this region that tends to increase both the upper and lower level temperatures. Similarly, the west coast is relatively cold with upwelling and $V > 0$.

The solution with damping included is qualitatively similar. At the east coast

$$T_E = T_0 + G(t) + K\int_0^t G(t')dt', \qquad (3.7)$$

where

$$G(t) = \int_0^t F_0(y - Ct')W(t, t'; K)dt'$$

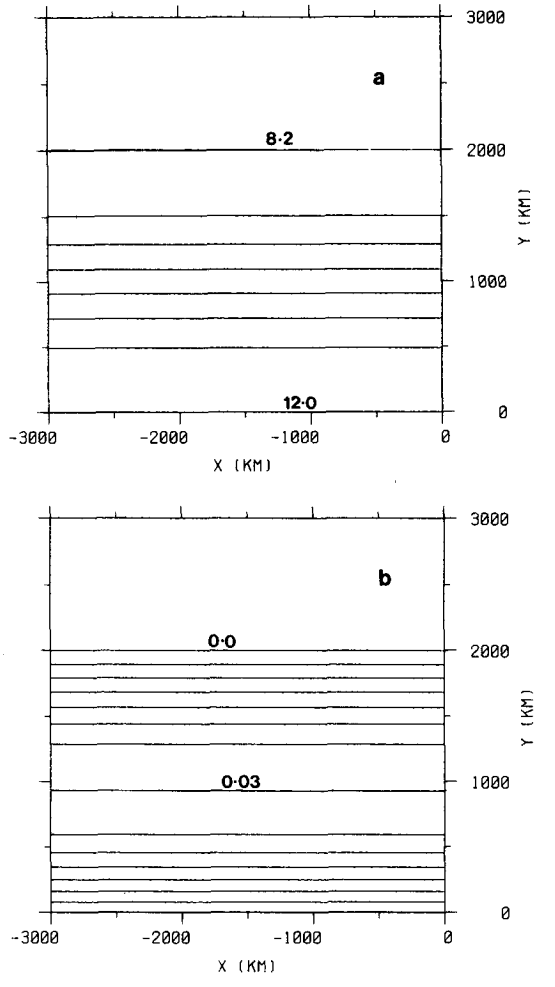

FIG. 3. The zonally uniform (no coast) response after 2000 days, Contour interval = (maximum − minimum)/7. (a) Upper level temperature T_1 (equal to surface temperature T_T for cooling); minimum = 8.2°C, maximum = 12°C. (b) Zonal velocity $U = u_1 - u_2$; minimum = 0.0, maximum = 0.03 m s^{-1}.

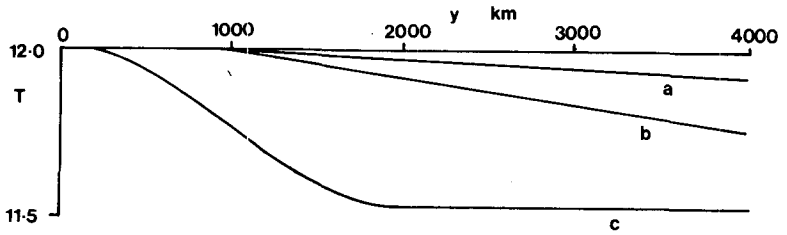

FIG. 4. Meridional sections of intermediate temperature T_I after 100 days with $F_1 = (T_A - T_{10})/\tau$, $F_2 = 0$ (no feedback): (a) at east coast with no damping ($K = 0$), (b) at east coast with $K = 1.2 \times 10^{-6}$ s^{-1} = 0.1 day^{-1}, and (c) the local (interior, no-coast) response $T_L = T_0 + F_0 t$.

with weight function

$$W(t, t'; K) = \exp(-Kt/2) I_0[\tfrac{1}{2}K(t^2 - t'^2)^{1/2}],$$

$$0 \leqslant t' \leqslant t.$$

(I_0 is a modified Bessel function, and $W \leqslant 1$, decreasing as t or t' increases.) Information carried by Kelvin waves is now altered by the damping: it is effectively lost on a length scale C/K. For a damping time of $K^{-1} = 10$ days this scale is about 2000 km.

Longshore profiles of T are shown in Fig. 4. Initially $T_1 = T_A(y_S)$ so there is cooling north of y_S, and $T_2 = T_B$. Changes along the coast are smallest for $K = 0$ (Fig. 4a), increasing as damping is increased to $K = 0.1$ day^{-1} (Fig. 4b). As $K \to \infty$, T_E approaches T_L (Fig. 4c), which increases linearly in time. Corresponding time profiles at $y = 2000$ km can be seen in Figs. 5b, 5c. With no damping or feedback T reaches a steady value at time $t = y/C$, but with $K > 0$ the magnitude of T_E continues to increase.

When forcing does not vary upstream from some point there are no longshore gradients to drive Kelvin waves and the response is local right up to the coast.

b. Spin-up with feedback in F

For $t \gtrsim \tau$ we should allow the surface heat flux to vary as T_1 changes. (The slower forcing F_2 is still neglected for $t \ll \mathcal{T}$.) The solution with

$$F = (T_A - T_1)/2\tau$$

is complicated. However we can simplify by using the approximation

$$T_1 = 2T - T_2 \approx 2T - T_B,$$

giving

$$F \simeq (T_A + T_B - 2T)/2\tau. \tag{3.8}$$

(This is reasonable while changes in T_2 are small.)

With this assumption (3.1) is again an equation for T alone, and can be easily solved. On the east coast

$$T_E = T_0 + \int_0^t F_0(y - Ct') W(t, t'; \tau^{-1}) dt'. \tag{3.9}$$

The weight W is the same as that for the damped case (3.7), but with τ^{-1} replacing K. Information is now altered by the ocean–atmosphere heat flux feedback. The long time scale ($\tau \gg K^{-1}$) implies a very large longshore decay distance $C\tau$. The time-dependent response with feedback can be seen in Fig. 5a. After a rapid initial increase the magnitude of T_E at $y = 2000$ km slowly decreases, in contrast to the damped no-feedback result in Fig. 5c.

We also find that the offshore decay scale decreases with time in this case, whereas it tends to increase in the model with damping and no feedback.

c. Steady state with damping and feedback

The time-dependent case with damping and feedback does not have such simple solutions. The steady state can be easily found, however, and is worth investigating. With benthic forcing included we use

$$\left.\begin{aligned} F_1 &= (T_A - T_1)/\tau \\ F_2 &= (T_B - T_2)/\mathcal{T} \end{aligned}\right\}.$$

The steady form of (2.11) requires

$$H_1 F_1 = H_2 F_2. \tag{3.10}$$

Then (3.1) leads to

$$-KL^2 T_{xx} + \gamma T = \gamma T_L, \tag{3.11}$$

where

$$\gamma = 1/[\delta\mathrm{T} + (1 - \delta)\tau],$$

$$T_L = \tfrac{1}{2}(T_A + T_B).$$

Near the east coast the solution to (3.11) takes the form

$$T = T_L[1 - \exp(-X)] + T_E \exp(-X)$$

with

$$X = (x_E - x)/D.$$

The compromise between damping and feedback gives an offshore decay scale

$$D = L(K/\gamma)^{1/2},$$

which is generally much larger than L. The reason for this increase in offshore scale is that the lower level balance between downwelling and benthic forc-

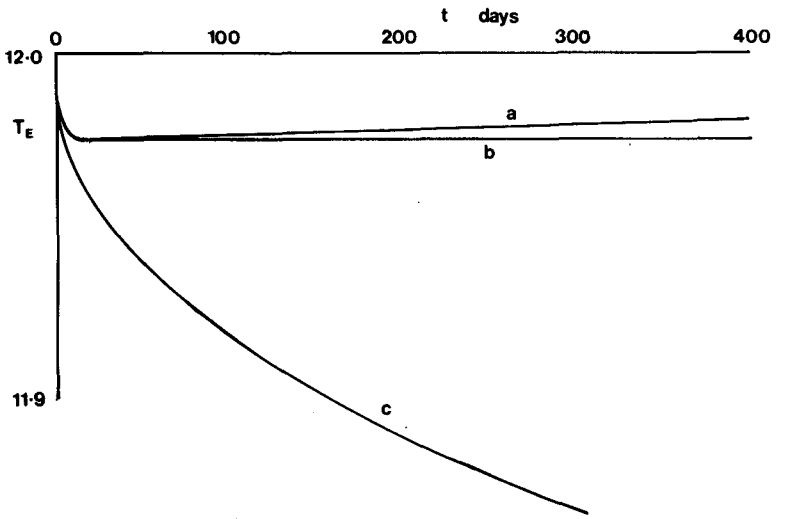

FIG. 5. Time dependence of T_I at east coast, at y = 2000 km: (a) feedback, no damping [$F = (T_A + T_B - 2T)/2\tau$, $K = 0$], (b) no feedback, no damping [$F = (T_A + T_B - 2T_0)/2\tau$, $K = 0$], and (c) no damping, no feedback [$F = (T_A + T_B - 2T_0)/2\tau$, $K = 0.1$ day^{-1}].

ing requires weak w_I, which in turn demands small V and T_x.

At the east coast,

$$T_E = T_E(y_S)\exp[-(y - y_S)/\lambda] + \lambda^{-1}\int_{y_S}^{y}\exp[-(y - y')/\lambda]T_L(y')dy', \quad (3.12)$$

where the large longshore scale is

$$\lambda = Df_0/K.$$

Another condition is needed. With forcing constant south of y_S we have

$$T_E(y_S) = T_L(y_S) \quad (3.13)$$

to complete the picture.

From (3.10), S can be found once T is known. It is useful to rearrange (3.10) as

$$S = S_L - A_2(T - T_L), \quad (3.14)$$

where

$$S_L = \tfrac{1}{2}(T_A - T_B),$$

$$A_2 = [\delta\mathrm{T} - (1 - \delta)\tau]/[\delta\mathcal{T} + (1 - \delta)\tau].$$

At the east coast $T_E > T_L$, so for $A_2 > 0$ we have $S_E < S_L$ and the static stability decreases poleward faster than for the open ocean. [Note that when $A_2 = 0(H_1\mathrm{T} = H_2\tau)$ the static stability does not depend on T.]

One limitation of this linear model becomes apparent. The effective atmospheric temperature T_A can decrease poleward sufficiently to drive $T_1 < T_2$. At this point deep convection should occur—an event not accounted for in this model. (We expect nonlinear effects to increase the static stability, however. For example, small g' implies small Rossby radius and decreased longshore decay scale, allowing T to vary more rapidly along the coast.)

The main points to note from this section are the tendency for Kelvin waves to warm the east coast and cool the west, and the large longshore scale for T. In the next sections this latter property is used to simplify the boundary conditions when considering Rossby waves.

4. Linear Rossby waves with no feedback

On a β-plane, with $\mathcal{D} = 0$ and no feedback, the linearized temperature equation (2.10a) becomes

$$T_t - L^2(T_{xxt} + \beta T_x) = F_0. \quad (4.1)$$

This case is similar to the wind-driven spin-up analyzed by Anderson and Gill (1975), henceforth referred to as *AG*. [See also McCreary (1976) for an analytic solution of a wind-driven two-layer equatorial β-plane model with Rossby and Kelvin waves.] The local response is modified by Rossby waves propagating away from the coasts. As described by AG, the eastern region is dominated by the longest and fastest Rossby waves, which have westward group and phase speed

$$c = \beta L^2,$$

typically 1 km day^{-1}, decreasing poleward. Waves travelling from the west coast with eastward group velocity are much shorter and slower, the maximum group velocity being $c/8$. Consequently most of the ocean is modified by information from the eastern

boundary only. The boundary condition $U = 0$ requires

$$fT_y + T_{xt} = 0, \quad \text{on} \quad x_E, x_W, \tag{4.2}$$

which provides some differences from AG, and some difficulties. Given T at the coasts, (4.1) can be easily solved at any particular latitude—but at x_E and x_W, T is controlled by Kelvin waves that couple different latitudes. This complication was overcome by AG by freezing $f(f = f_0, f_y = \beta)$ to obtain

$$f_0^2 U = -(\beta\phi^* + f_0\phi_y^* + \phi_{xt}^*), \tag{4.3}$$

where

$$f\phi^* = \tfrac{1}{2}H\alpha g f_0(T - T_0) = f_0\phi.$$

By decomposition into sinusoidal meridional modes they then construct an equation for U of the form (4.1), which can be solved with $U = 0$ at the coasts. [On an equatorial β-plane McCreary (1976) uses Hermite function meridional modes.]

Unfortunately (4.3) is not appropriate to the thermally forced problem because U should only be driven by temperature gradients. For example, spatially constant F should change T uniformly with no associated currents. [Note that (4.3) is suitable for purely wind-driven models because such forcing does not generate uniform T changes.] Moreover, as shown in Appendix C, the corresponding equation for ϕ^* has an unstable free mode associated with Kelvin waves with $U \equiv 0$.

With boundary conditions (4.2) this model cannot be reduced to a two-dimensional (x, t) problem. However, because coastal Kelvin waves are much faster than Rossby waves, we can expect T to be almost uniform along the coasts and determined by upstream conditions. Approximate boundary conditions are

$$\left.\begin{aligned} T_E &= T(y_S, t) \\ T_W &= T(y_N, t) \end{aligned}\right\}. \tag{4.4}$$

Then Kelvin waves effectively travel instantly, and (4.1) represents a slow-time model for the development of Rossby waves.

For forcing, which is constant south of y_S and north of y_N, we have

$$T_E = T_0 + F_0(y_S)t, \tag{4.5a}$$

$$T_W = T_0 + F_0(y_N)t. \tag{4.5b}$$

In the interior, where waves have not yet arrived, the local response is

$$T_L = T_0 + F_0 t. \tag{4.5c}$$

For the western region, the Lighthill (1969) approximate solution used by AG leads to

$$T = T_L + (T_W - T_L)[\beta(x - x_W)t]^{-1/2}J_1(Z), \tag{4.6}$$

where

$$Z = 2[(x - x_N)ct - (x - x_W)^2]^{1/2}L^{-1},$$

and J_1 is a Bessel function. This region slowly broadens, but it contains a thinning boundary layer next to the coast set up by the dispersion of short Rossby waves. The zonal gradient at x_W is

$$T_x = -\tfrac{1}{2}[1 + (ct/L)^2](T_W - T_L)/ct. \tag{4.7}$$

(For small t, $T_W - T_L$ is proportional to t.) In the absence of damping, T_x grows rapidly and unrealistically large longshore velocities soon appear, so the analytic western solution (4.6) is actually of limited use. Note that V is positive at the coast when $T_W < T_L$.

On the east side non-dispersive long Rossby waves dominate, giving

$$T = T_L + (T_E - T_L)[1 - (x_E - x)/ct] \tag{4.8}$$

for $x_E - ct \leq x \leq x_E$. The zonal gradient in this region is

$$T_x = (T_E - T_L)/ct \tag{4.9a}$$

which is independent of x, and the meridional gradient is

$$T_y = [T_{Ly} - (T_E - T_L)2\beta/f](x_E - x)/ct. \tag{4.9b}$$

The $T_E - T_L$ term in (4.9b) is due to latitude dispersion of the Rossby waves. At the wavefront $x = x_E - ct$ the discontinuity in ∇T (and hence in U, which is geostrophic for these long waves) is smoothed out by short waves in practice. When $T_E > T_L$ we find $V > 0$, and there is downwelling accompanying the divergence $\nabla \cdot \mathbf{U}$.

Our standard atmospheric temperature distribution (2.16) leads to a broad relatively warm eastern region and a cold narrow western boundary layer. The eastern region after 2000 days is illustrated in Fig. 6. The upper level temperature in Fig. 6a is negative in the north, with $T_1 < T_2$, because the amplitude of the response to the surface cooling is too large when there is no feedback. However the pattern is of interest, and can be rescaled (see below). Compared to the no-coast result in Fig. 3a the water near the east coast is much warmer, principally due to the "instant" Kelvin wave. The lower level temperature T_2 is driven only by downwelling, and slight warming in the wave region can be seen in Fig. 6b. (The variation of Rossby wave speed with latitude shows clearly in this diagram.) Note that T_1 and T_2 are not constant along the coast, in contrast to T. Geostrophic velocities are mapped in Figs. 6c, 6d. In the interior U is purely zonal, corresponding to Fig. 2b. There is a jump in U and V at the wavefront, behind which V is zonally constant and increases poleward. U decreases linearly to vanish at the coast.

Zonal sections of T, with the west coast included,

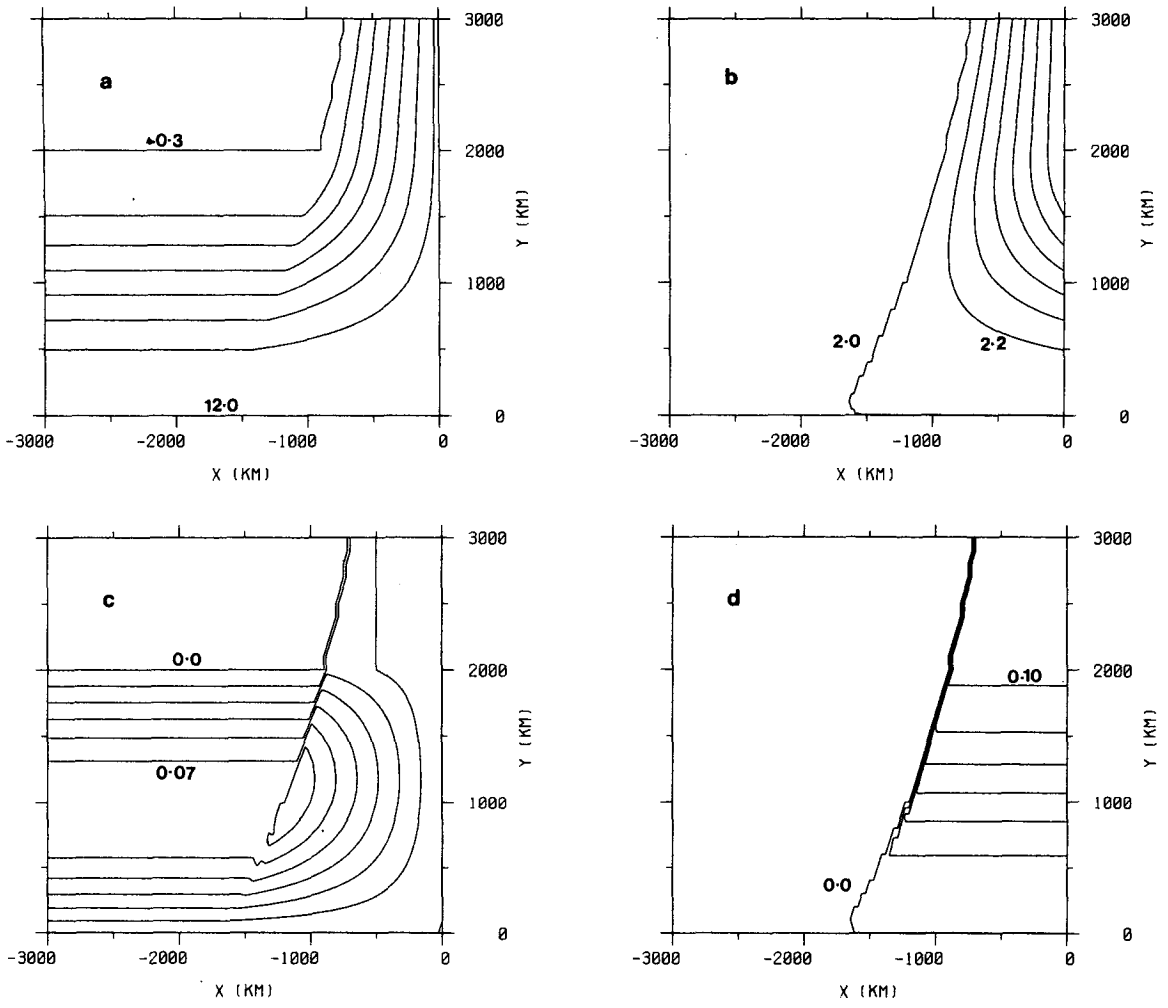

FIG. 6. Eastern region spinup by long Rossby waves, after 2000 days with $F_1 = (T_A - T_{10})/\tau$, $F_2 = 0$ (no feedback) and $T_E = T_L(y_S) = 7°C$ (instant undamped Kelvin waves): (a) upper level temperature T_1, min = −0.3, max = 12°C; (b) lower level temperature T_2, min = 2.0, max 3.3°C; (c) zonal velocity U, min = 0.0, max = 0.10 m s^{-1}; (d) meridional velocity V, min 0.0, max 0.12 m s^{-1}.

are plotted in Fig. 7a, at $y = 0$, 1000 and 2000 km. Though the western wave region is over 100 km wide after 2000 days, the western boundary layer has effectively thinned to about 5 km width. The enlargement in Fig. 7b shows the very abrupt transition from the interior value of T to the relatively cold coastal value T_W. Steady results in Section 6 show how inclusion of damping limits this thinning.

The temperature changes described in this section are unreasonably large because feedback has been neglected. A simple but crude way of improving the magnitude of the response is to replace T_E, T_W and T_L by, for example,

$$T_L = T_0 + F_0\tau[1 - \exp(-t/\tau)].$$

This gives a no-coast interior agreeing with Fig. 3, and also gives $T_1 > T_2$ everywhere.

The pattern as well as the magnitude should be changed because the Rossby waves travel slowly and are themselves modified while moving away from the coast, and in the next section the large eastern region is examined in more detail. (Note though that the *net* meridional transport in the eastern and western regions depends only on $T_E - T_L$ and $T_W - T_L$, respectively.)

5. The eastern region and long Rossby waves

In this section we investigate the effects of nonlinearity and feedback on the long Rossby waves that control the eastern region. For these waves with wavelength much larger than the Rossby radius the velocity is geostrophic:

$$f(U, V) = \tfrac{1}{2}H\alpha g(-T_y, T_x).$$

Then the divergence is simply

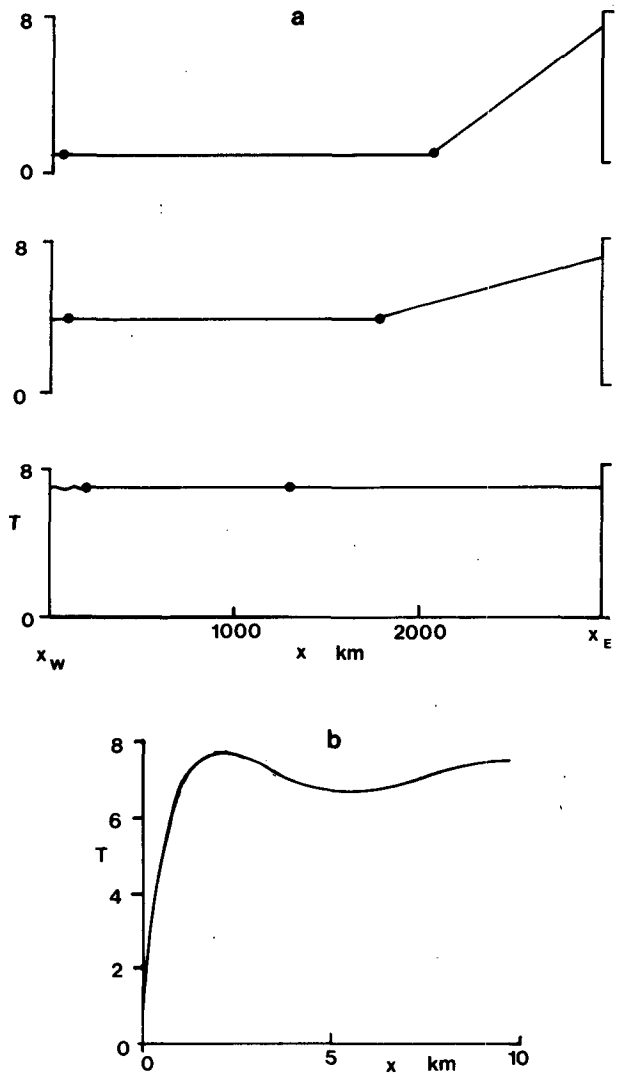

FIG. 7. Zonal sections of T_l corresponding to Fig. 6, with west coast added. (a) Sections across basin at $y = 0$, 1000 and 2000 km. Circles indicate positions $x_W + ct/8$, $x_E - ct$. (b) Enlargement of region near west coast, at $y = 0$ km.

$$\nabla \cdot \mathbf{U} = -\beta V/f, \tag{5.1a}$$

and advection of T vanishes,

$$\mathbf{U} \cdot \nabla T = 0, \tag{5.1b}$$

because $f\mathbf{U}$ follows contours of T.

Using (5.1) the temperature equation (2.9a) can be written

$$T_t - c(1 + S'/S_0)T_x + \tfrac{1}{2}\mathbf{U} \cdot \nabla S' = F, \tag{5.2}$$

where S' is the stratification change from the constant initial value S_0, and the initial longwave speed is

$$c = \tfrac{1}{4}\beta\alpha g S_0 H/f^2 = \beta L^2.$$

The nonlinear terms in (5.2) represent modification of the long-wave speed by changing static stability and horizontal advection of S. With no T advection we also have

$$[S - (1 - 2\delta)T]_t = \delta F_1 - (1 - \delta)F_2, \tag{5.3}$$

which is equivalent to (2.11). As in the previous section, instant Kelvin waves give T constant along the east coast.

a. Linear spinup with surface feedback

We first examine the effect of feedback by using

$$\left.\begin{aligned} F_1 &= (T_A - T_1)/\tau \\ F_2 &= 0 \end{aligned}\right\},$$

and the linear version of (5.2):

$$\begin{aligned} T_t - cT_x &= F \\ &= (T_A - S - T)/2\tau. \end{aligned} \tag{5.4}$$

Eliminating S from (5.3) and (5.4) leads to

$$\tau(T_t - cT_x)_t + T_t - \delta c T_x = 0 \tag{5.5}$$

to be solved subject to the initial conditions

$$\left.\begin{aligned} T_t - cT_x &= (T_A - T_{10})/2\tau \\ T &= T_0 \end{aligned}\right\}$$

at $t = 0$. When $T_A = T_{10}$ south of y_S, the coastal condition is simply

$$T_E = T_0.$$

West of the wavefront at $x_E - ct$ the response is still local, with

$$\begin{aligned} T_L &= T_0 \exp(-t/\tau) + \tfrac{1}{2}(T_A + T_B)[1 - \exp(-t/\tau)] \\ &= T_0 + \tfrac{1}{2}\Delta[1 - \exp(-t/\tau)], \end{aligned} \tag{5.6a}$$

$$T_2 = T_B, \tag{5.6b}$$

where

$$\Delta = T_A - T_{10} = T_A - T_A(y_S).$$

(Note that Δ is negative for T_A decreasing northward.)

In the wave-modified region $x_E - ct \leqslant x \leqslant x_E$, (5.5) can be solved using Laplace transforms to obtain

$$\begin{aligned} T = T_L - \tfrac{1}{2}\Delta \exp(-X)[1 - \exp(-W) \\ + \int_0^W [1 - \exp(W' - W)] \exp(-\delta W') \\ \times (\delta X/W')^{1/2} I_1(2\sqrt{\delta X W'}) dW', \end{aligned} \tag{5.7}$$

where

$$\begin{aligned} X &= (x_E - x)/D, \\ D &= c\tau/(1 - \delta), \\ W &= (ct + x - x_E)/c\tau. \end{aligned}$$

W varies linearly from 0 at the wavefront to t/τ at the coast. The lower level temperature is

$$T_2 = T_B - \delta\Delta \exp(-X) \int_0^W \exp(-\delta W') \times I_0(2\sqrt{\delta X W'})dW'. \quad (5.8)$$

(I_0 and I_1 are modified Bessel functions.) As $\tau \to \infty$ in these expressions the no-feedback result (4.8) is regained.

The solution looks complicated but two important features can be recognized. The main one is the term $\exp(-X)$ which causes offshore decay of the information carried by the Rossby waves. The physical explanation of this behavior can be traced to the more rapid cooling of places with larger upper-level temperature. This tends to decrease T gradients and counteracts the generation of zonal gradients by the Rossby waves travelling from the coast. The timescale τ and the wavespeed c determine the decay scale D, which is typically about 500 km.

Near the coast the results simplify to reveal another feature. At $x = x_E$ we find

$$T_2 = T_B - \Delta[1 - \exp(-\delta t/\tau)], \quad (5.9a)$$

$$T_1 = T_{10} \exp(-\delta t/\tau) + T_A[1 - \exp(-\delta t/\tau)], \quad (5.9b)$$

$$V = -(\Delta f/S_0\beta\tau) \exp(-\delta t/\tau). \quad (5.9c)$$

A long time scale τ/δ appears. After the initial Rossby wave spinup there is further slow adjustment as downwelling changes the benthic temperature, which in turn affects T and V. Offshore regions are similarly affected, with weaker downwelling beginning after the wavefront passes. With no benthic forcing to limit the change in T_2, (5.9) gives $T_2 \to T_B - \Delta$, $T_1 \to T_A$, and $V \to 0$ at the coast for $t \gg \tau/\delta$. (As in Section 3, there is a problem with $T_1 < T_2$ if Δ is sufficiently large.)

The response to atmospheric forcing [(2.16)] after 2000 days is shown in Fig. 8, and can be compared

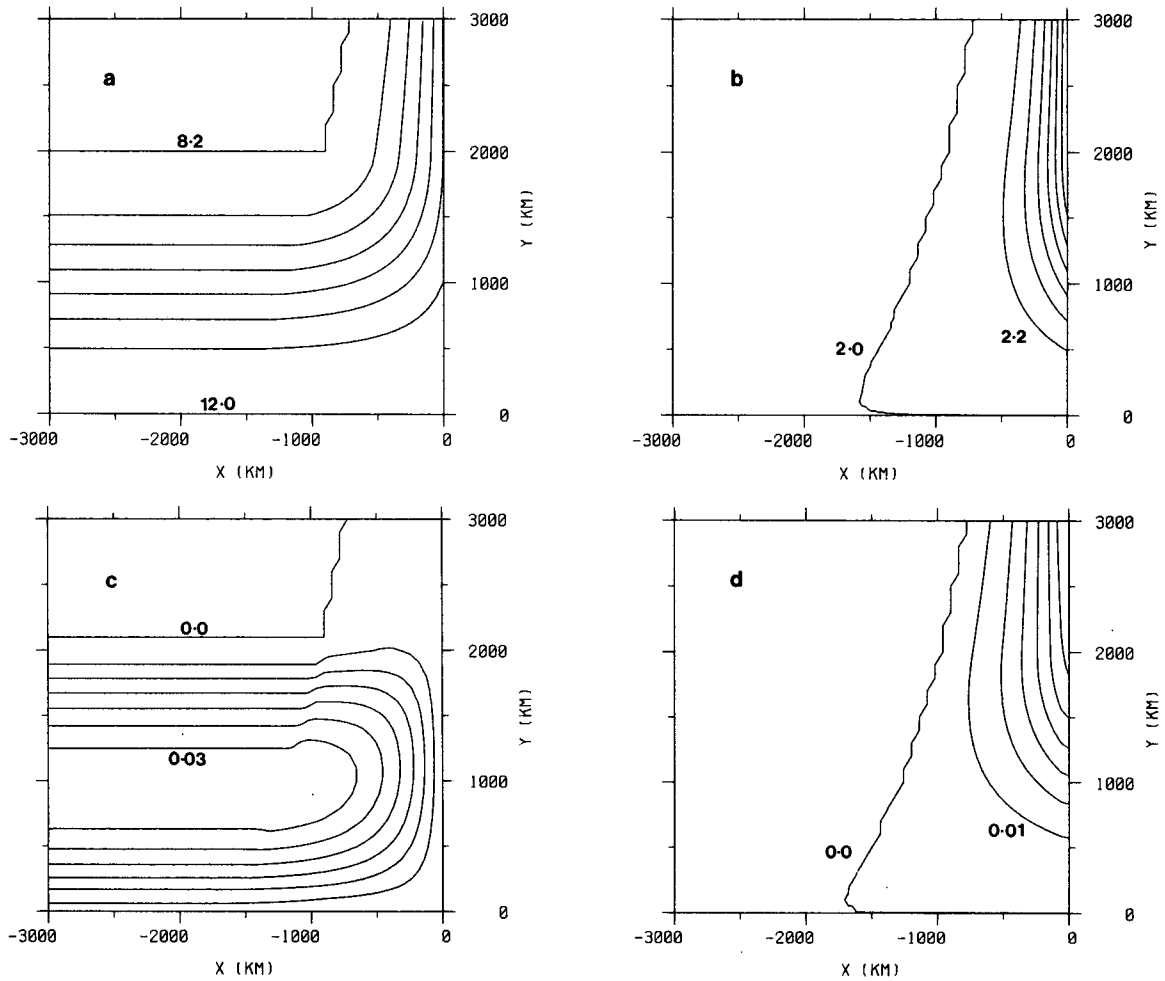

FIG. 8. Eastern region spinup by long Rossby waves, after 2000 days with $F_1 = (T_A - T_1)/\tau$, $F_2 = 0$ (as for Fig. 6, but with feedback): (a) T_1, min = 8.2, max = 12°C; (b) T_2, min = 2.0, max = 3.1°C; (c) U, min = 0.0, max = 0.03 m s^{-1}; (d) V, min = 0.0, max = 0.08 m s^{-1}.

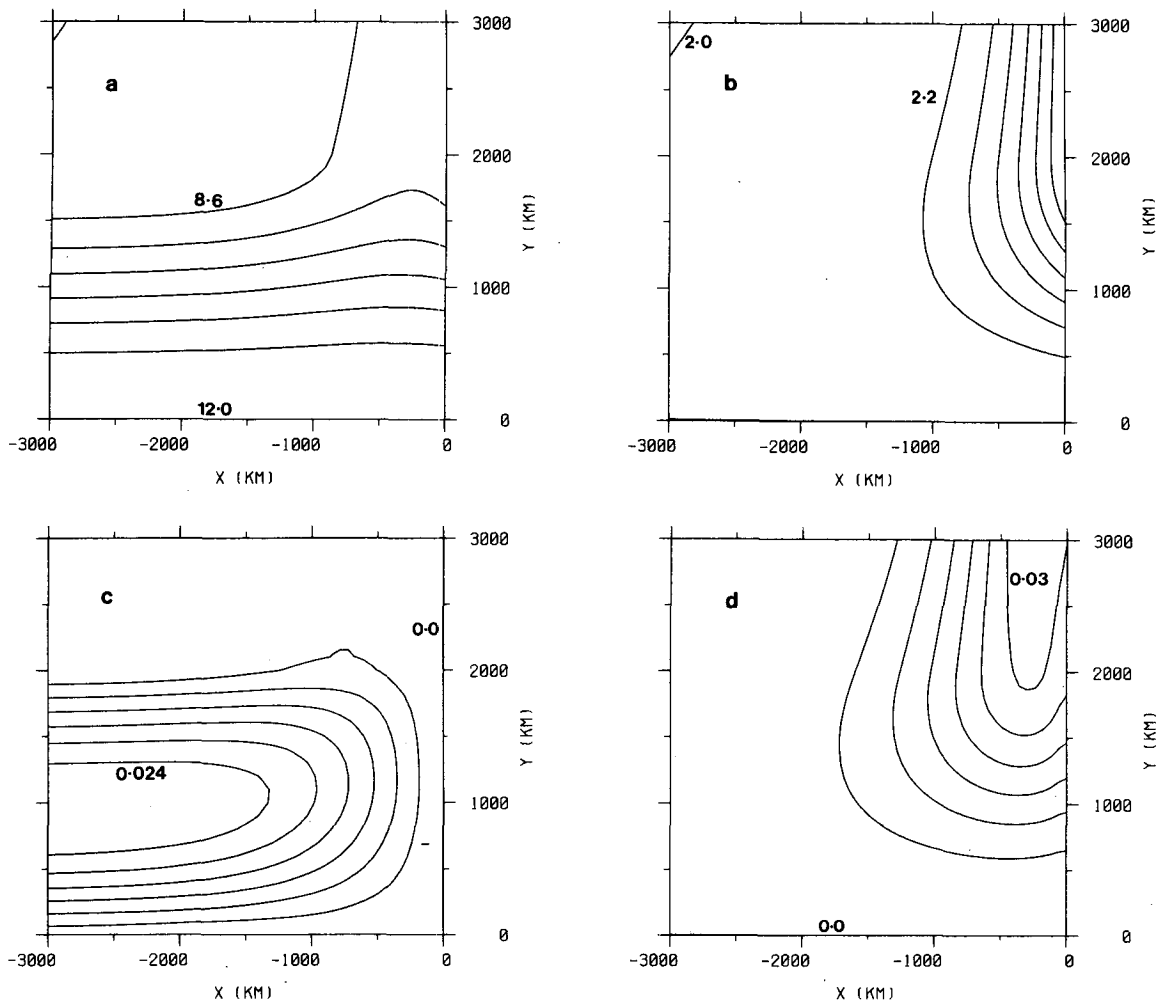

FIG. 9. As for Fig. 8, but at t = 10 000 days: (a) T_1 = 8–12°C, (b) T_2 = 2.0–3.2°C, (c) U = 0.0–0.03 m s^{-1}, and (d) V = 0.0–0.03 m s^{-1}.

with the patterns without feedback in Fig. 6. The contrast is most striking in the V-field, which now decays offshore instead of remaining constant between the coast and the wavefront. Zonal sections of T in Fig. 10 show the same decay, and the relation between wavespeed and offshore decay scale is clear (cf. Fig. 7 without feedback). Fig. 9 gives results after 10 000 days. By this time the V-maximum has moved slightly offshore as downwelling slowly increases T_2. Note that the surface temperature T_1 has almost relaxed to T_A. The zonal sections of T in Fig. 10 show also that the decay scale is slowly increasing with time in this case. After a very long time $T \rightarrow T_E$ at any point offshore.

b. Spinup with strong benthic forcing and nonlinearity

The general nonlinear equation is difficult to solve explicitly, but simple results can be obtained for

$$F_2 = (T_B - T_2)/\tau, \tag{5.10}$$

giving

$$F = (T_A + T_B - 2T)/2\tau.$$

This represents strong damping of lower level temperature. However, because changes in T_2 are slow—zero in the interior—this overestimate of benthic forcing should have little effect until $t \gg \tau$. The local

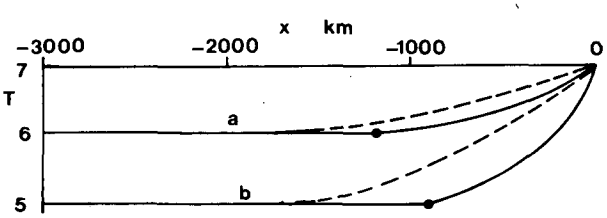

FIG. 10. Zonal sections of T_1 corresponding to Figs. 8, 9 at (a) y = 1000 km, (b) y = 2000 km after 2000 days (solid) and 10 000 days (dashed). Circles indicate position of Rossby wavefront.

response is still (5.6). Further, this strong forcing case complements the above example with $F_2 = 0$.

We can solve (5.3) immediately to obtain the diagnostic

$$S' = (1 - 2\delta)(T - T_0) + \delta\Delta[1 - \exp(-t/\tau)]$$
$$= (1 - 2\delta)(T - T_L) + \tfrac{1}{2}\Delta[1 - \exp(-t/\tau)]. \quad (5.11)$$

The advection term consequently reduces to

$$\mathbf{U}\cdot\nabla S' = V\delta T_{Ay}[1 - \exp(-t/\tau)]$$
$$= -2\delta U_L T_x, \quad (5.12)$$

where U_L is the zonal velocity driven by T_L. Then (5.2) becomes

$$T_t - c(1 + S'/S_0)T_x - \delta U_L T_x = F. \quad (5.13)$$

With $T_{Ay} < 0$ we have $U_L > 0$ and advection is effectively *increasing* the westward wavespeed. *A priori* one might expect a decrease in wavespeed due to UT_x, but this term is cancelled by VT_y because $\mathbf{U}\cdot\nabla T = 0$. A similar effect was described by Anderson and Killworth (1979) in their analysis of nonlinear wind-driven long Rossby waves.

As described in Appendix D, Eq. (5.13) together with (5.11) can be solved using characteristics. Before presenting some nonlinear results, however, we can first solve the simpler equation

$$T_t - cT_x = F$$

to compare with the earlier $F_2 = 0$ case. In this linear limit the wavefront is again at $x_E - ct$, and in the wave region

$$T = T_L - \tfrac{1}{2}\Delta \exp(-(x_E - x)/c\tau)$$
$$\times [1 - \exp(-W)], \quad (5.14a)$$

$$T_2 = T_B - \delta\Delta \exp(-(x_E - x)/c\tau)$$
$$\times [1 - \exp(-W)], \quad (5.14b)$$

$$V = (\Delta f/S_0\beta\tau) \exp(-(x_E - x)/c\tau), \quad (5.14c)$$

where $W = (ct + x - x_E)/c\tau$ as in (5.7). Compared to the $F_2 = 0$ result, the offshore decay scale is reduced by the factor $1 - \delta$ to $c\tau$ and the long time scale τ/δ is suppressed by the benthic forcing. For the usual T_A distribution the response after 2000 days is very similar to that shown in Fig. 8 for $F_2 = 0$. Note that V is steady behind the wavefront. If the benthic timescale were larger than τ then there would be further slow adjustment.

Results with nonlinear terms retained are given in Fig. 11 for $t = 2000$ days. The wavefront is at

$$x = x_E - c[(1 + \mu)t - \mu\tau[1 - \exp(-t/\tau)]], \quad (5.15)$$

where

$$\mu = (\Delta - 2\delta T_{Ay} f/\beta)/2S_0.$$

At the higher latitudes where T_A is independent of y the long waves are appreciably slowed by the reduced static stability there, and the coastal influence decays rapidly offshore. Further south, where $T_{Ay} < 0$, advection outweighs the decrease in S and the wave speed is effectively increased. Despite changes of up to 50% in S, however, the linear and nonlinear results are not all that different. This is mainly because T is fixed at the coast and there is offshore decay to the same interior in each case. More contrast can be expected when T_A is time-dependent (seasonal variations, for example). Zonal sections of T at $y = 1000$ and 2000 km, and $t = 2000$ and 10 000 days, are given in Fig. 12, and can be compared with those in Fig. 10.

c. *Steady nonlinear long waves*

The long-wave model has a simple steady state. For forcing

$$\left.\begin{aligned} F_1 &= (T_A - T_1)/\tau \\ F_2 &= (T_B - T_2)/\tau \end{aligned}\right\},$$

we have from (5.3)

$$S = S_L - A_2(T - T_L), \quad (5.16)$$

where the local values T_L and S_L and the constant A_2 are the same as for the steady f-plane model in Section 3. With $\mathbf{U}\cdot\nabla T$ vanishing, the steady form of the temperature equation (2.9a) reduces to

$$\tfrac{1}{2}\nabla\cdot(\mathbf{U}S) = F$$
$$= -\gamma(T - T_L), \quad (5.17)$$

where γ is the inverse time scale defined in Section 3.

Using the divergence (5.1a) and substituting for S from (5.16), Eq. (5.17) becomes an equation for $T - T_L$, i.e.,

$$-c_L[1 - A_2(T - T_L)/S_L + A_1](T - T_L)_x$$
$$+ \gamma(T - T_L) = 0. \quad (5.18)$$

Here

$$A_1 = -(S_L + A_2 T_L)_y f/\beta S_L,$$

and $c_L = \beta g'_L H/f^2$ is the long-wave speed for the local stratification S_L. The terms involving A_1 and A_2 represent modifications of this speed by advection and varying static stability, similar to the special spinup case above.

With the boundary condition $T = T_E$ at $x = x_E$, Eq. (5.18) can be solved at any particular latitude to obtain

$$(T - T_L) \exp[-(T - T_E)A_2 c_L/S_L a]$$
$$= (T_E - T_L) \exp[-(x_E - x)\gamma/a], \quad (5.19)$$

where

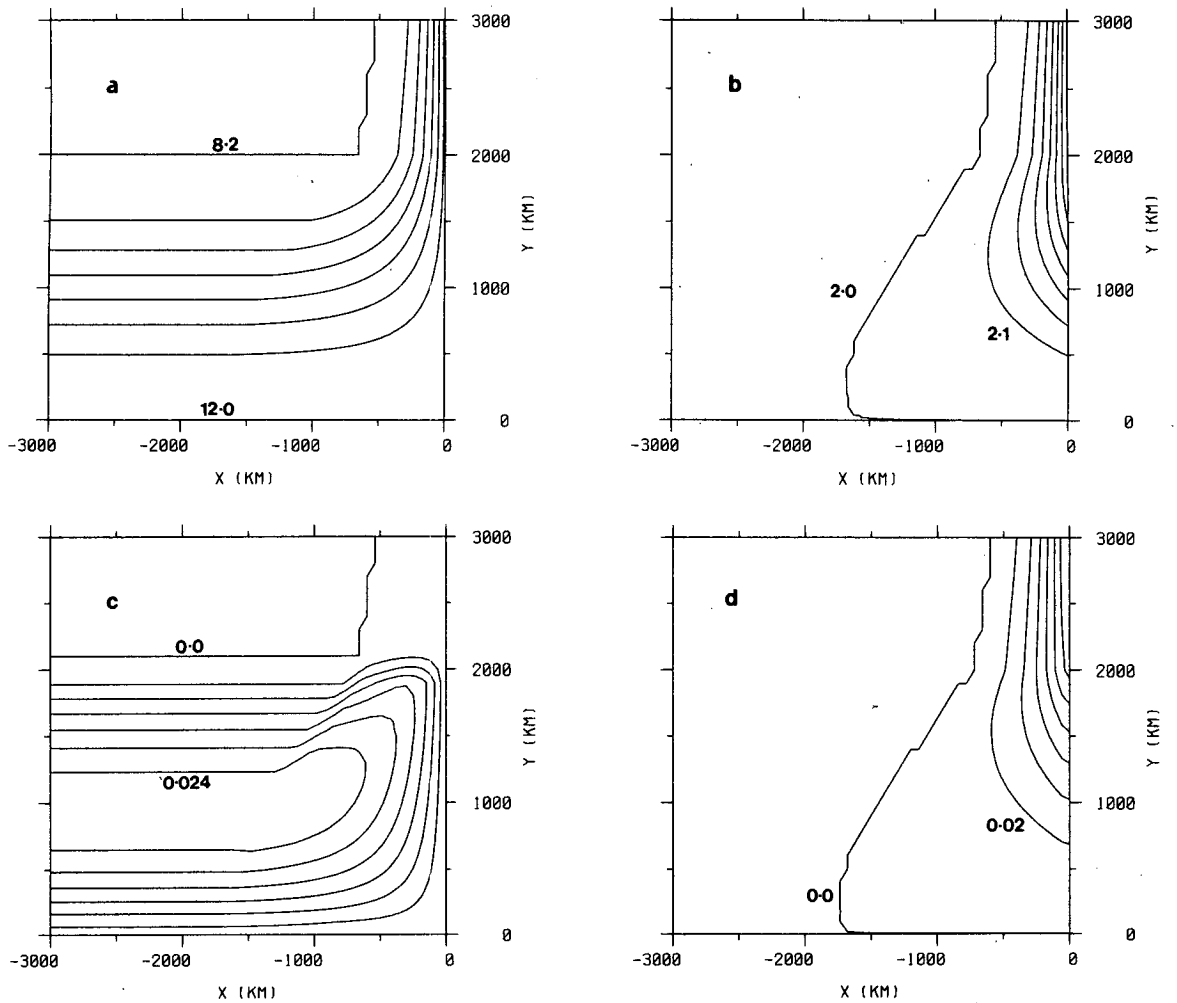

FIG. 11. Eastern region spinup by long nonlinear Rossby waves, after 2000 days with $F_1 = (T_A - T_1)/\tau$, $F_2 = (T_B - T_2)/\tau$, $\delta T = (1 - \delta)\tau$: (a) T_1 = 8.2–12°C, (b) T_2 = 2.0–2.4°C, (c) U = 0.0–0.03 m s^{-1}, and (d) V = 0.0–0.12 m s^{-1}.

$$a = c_L(1 + A_1)$$

is the advection-modified wavespeed. This is the speed of a wavefront advancing into stratification S_L when forcing varies with latitude. With $A_1 > 0$ (e.g., $T_{Ay} < 0$) relatively warm water is advected northward, effectively increasing the speed of warm information propagating from the east coast.

At x_E the westward decay scale is a/γ which is analagous to the scale $c\tau$ encountered earlier. If the benthic time scale $\mathbf{T}$ is increased then a/γ also increases because smaller T_x (proportional to w_I) is needed to balance F_2.

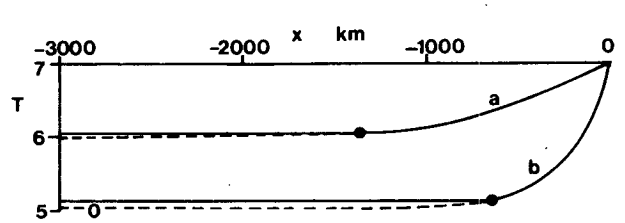

FIG. 12. Zonal sections of T_I for conditions as in Fig. 11, at (a) y = 1000 km, (b) y = 2000 km after 2000 d (solid) and 10 000 days (dashed). Circles indicate wavefronts.

In the next section more general steady models are investigated. The long-wave restriction is dropped, and damping/diffusion allows T to vary along the coast. West coast effects are also included.

6. Steady model with feedback and damping

Time-dependent results with damping as well as feedback are difficult to obtain analytically, so in this section only steady models are considered.

Using the notation established in Section 5.c, the steady nonlinear temperature equations (2.9) lead to

$$S = S_L - A_2(T - T_L) - A_3\mathbf{U}\cdot\nabla T, \qquad (6.1)$$

where

$$A_3 = 2\delta(1 - \delta)\tau\mathrm{T}/[\delta\mathrm{T} + (1 - \delta)\tau],$$

$$\tfrac{1}{2}\nabla\cdot(\mathbf{U}S) - \tfrac{1}{2}A_2U\cdot\nabla T + \gamma(T - T_L) = 0. \qquad (6.2)$$

Then substituting for S in (6.2) from (6.1) gives a (rather cumbersome) equation involving T alone.

From (2.8) we have

$$\tfrac{1}{2}H\alpha gU\cdot\nabla T = -V\mathcal{D}, \tag{6.3a}$$

$$f\nabla\cdot\mathbf{U} = -\beta V - \mathcal{D}_x. \tag{6.3b}$$

At the east and west coasts, vanishing U requires

$$\tfrac{1}{2}H\alpha gT_y + \mathcal{D} = 0. \tag{6.4}$$

As before, we use the corner conditions

$$\left.\begin{aligned} T(x_E, y_S) &= T_L(y_S),\\ T(x_W, y_N) &= T_L(y_N)\end{aligned}\right\}. \tag{6.5}$$

[There is an assumption here that the east (west) coast does not influence $T_L(y_S)(T_L(y_N))$. In more complete models with closed boundaries or an equatorial waveguide these boundary conditions are altered.]

a. Linear

When disturbances are small we omit $\mathbf{U}\cdot\nabla T$ and set $S = S_L$. [Effectively $\mathbf{U}\cdot\nabla S$ is replaced by $U_L S_x + VS_{Ly}$ in (6.2).] The simplified equations reveal the important zonal and longshore decay scales.

We first consider $\mathcal{D} = KV$, for which (6.3) reduces to

$$-KL^2T_{xx} - aT_x + \gamma T = \gamma T_L, \tag{6.6}$$

where a is the advection-modified long-wave speed defined in Section 5.c. [With $K = 0$, (6.6) reduces to the linear version of the long-wave equation (5.1), and when $a = 0$ in (6.6) the linear f-plane equation (3.11) is obtained.] The general solution of (6.6) can be expressed as

$$T = T_L + E(y)\exp[-(x_E - x)/D_E] + W(y)\exp[-(x - x_W)/D_W], \tag{6.7}$$

where

$$\left.\begin{aligned} D_E &= r a/\gamma, \quad D_W = KL^2/ar\\ 2r &= 1 + (1 + 4KL^2\gamma/a^2)^{1/2}\end{aligned}\right\}.$$

The dependence of D_E on K is very weak. Dynamically the eastern region is dominated by the long waves, which are governed by (6.6) with $K = 0$. The westerly decay scale D_W is bounded by K/β and is much smaller than D_E, being typically less than 100 km. This scale is important near the west coast and is due to a balance of damping and the thinning mentioned in Section 4. It depends only weakly on γ—Eq. (6.6) with $\gamma = 0$ is a reasonable approximation near the west coast. Note that

$$(D_E D_W)^{1/2} = L(K/\gamma)^{1/2}$$

which is the offshore decay scale found in Section 3 for the f-plane.

From (6.4)

$$T_y = -(K/f)T_x \tag{6.8}$$

at the coasts. Together with (6.5) this condition can be used to determine $E(y)$ and $W(y)$ analytically. More insight is gained by considering some approximate answers, however. Away from the western boundary $W(y)$ can be neglected and (6.7) and (6.8) lead to

$$T_E = T_L(y_S) + E = T_L(y_S) - \int_{y_S}^{y} (K/fD_E)E\,dy. \tag{6.9}$$

The longshore decay scale $D_E f/K$ is usually very large, so T is close to $T_L(y_S)$ along the east coast and the geostrophic approximation $T_E = T_L(y_S)$ is a good first guess. (This approximation breaks down if D_E becomes small, however, which happens when static stability decreases markedly.)

If $D_E \ll x_E - x_W$ then at the west coast we similarly have

$$T_W = T_L(y_N) + W = T_L(y_N) - \int_{y_N}^{y} (K/fD_W)W\,dy. \tag{6.10}$$

The western longshore decay scale $D_W f/K$ is shorter than its eastern counterpart and T_W can vary significantly. Note that

$$D_W f/K \leqslant f/\beta \approx 500 \text{ km}$$

and this scale has only weak K dependence. [Eq. (6.10) can be easily modified to include T_E effects when $D_E \gtrsim x_E - x_W$.]

Fig. 13 shows results for a model with $K = 0.1$ day^{-1} and $\mathcal{T} = (1 - \delta)\tau/\delta$ (i.e., $\mathcal{T} \approx 6000$ days). We see eastern region development similar to that found in the previous section, together with a narrow western boundary layer. The eastern zonal decay scale is clearest in the T_2 map. A strong T_{Ay} effect is evident, and this scale exceeds the basin scale in places. The T_1 map shows a relatively warm east coast, particularly at higher latitudes where D_E is smaller, and a cold west coast. The meridional velocity V is poleward everywhere, being strongest at the coasts, particularly on the western side. This can be inferred from the zonal sections of T given in Fig. 14, since V is proportional to T_x. The vertical velocity w_I in Fig. 13d reveals relatively strong upwelling near the west coast, with weak downwelling elsewhere. Where D_E is changing rapidly with latitude ($y \approx 2000$ km) there is an increase in U (Fig. 13c) sufficient to shift the maximum U substantially away from the U_L maximum at $y \approx 900$ km.

Due to the effect of T_{Ay} on a, the western boundary layer can be very narrow (less than 20 km in places in the example above) with associated large V. The same effect occurs when nonlinear terms are retained, and this causes a problem because the term $\mathbf{U}\cdot\nabla T$ can then drive an unphysically large increase in S. (This defect is due to the two-level truncation, which

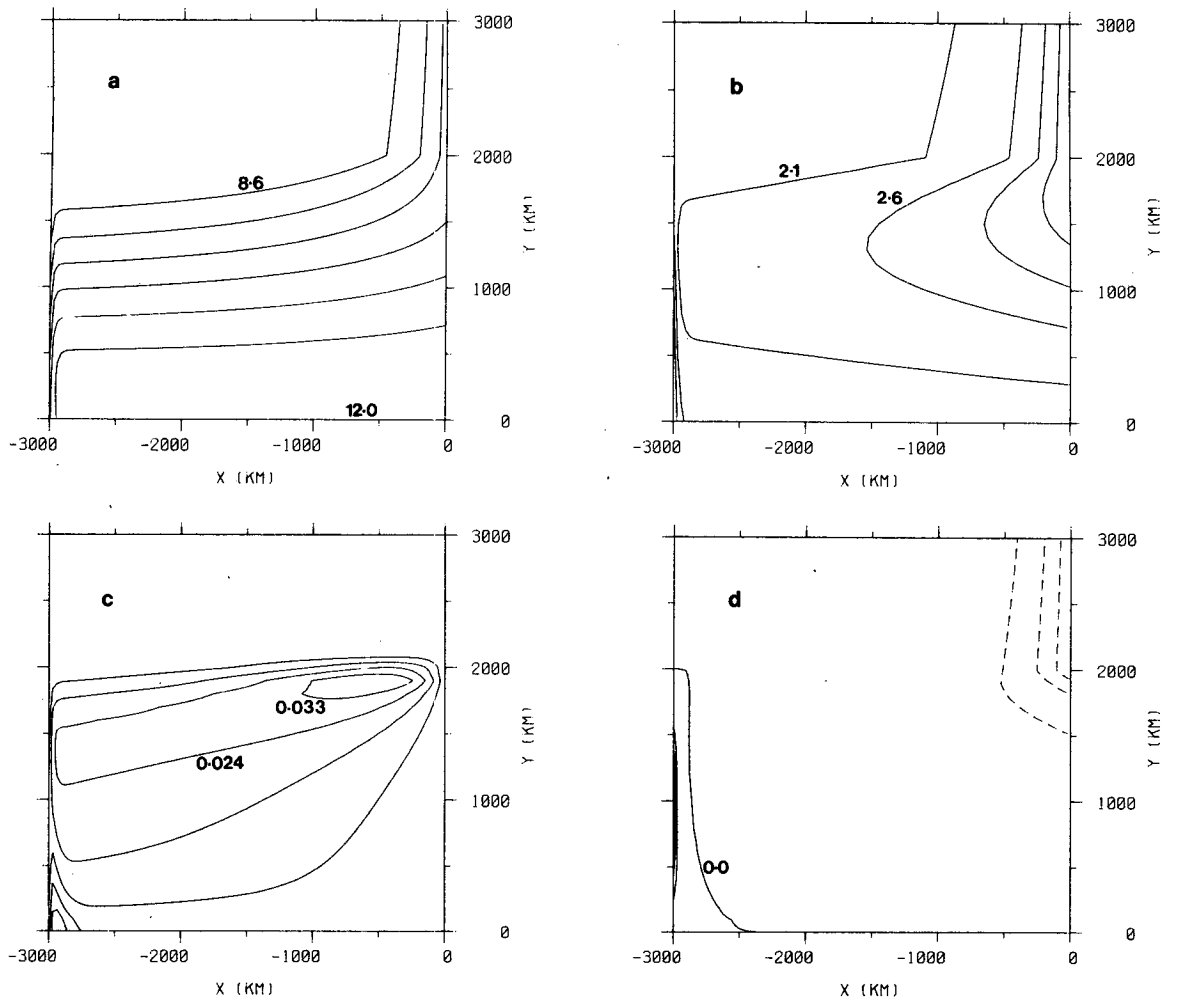

FIG. 13. Steady linear model with east and west coasts, $F_1 = (T_A - T_1)/\tau$, $F_2 = (T_B - T_2)/\mathrm{T}$, $\delta\mathrm{T} = (1 - \delta)\tau$, damping K = 0.1 day^{-1}: (a) T_1 = 8.0–12°C, (b) T_2 = 0.69–4.0°C, (c) U = 0.02–0.04 m s^{-1}, and (d) intermediate level vertical velocity $w_I = -3.6 \times 10^{-11}$ to 1.0×10^{-9} m s^{-1} (dashed contours for w_I have interval |min|/4, solid contours have interval max/4) [10^{-9} m s$^{-1} \approx 3$ cm year^{-1}].

is inadequate for such regions where we expect higher order vertical modes to be significant. Further, strong upwelling emphasizes the poor representation of vertical structure.) There are several ways of avoiding such narrow boundary layers. Increasing K reduces V, but makes D_W unreasonably large elsewhere. Nonlinear damping

$$\mathcal{D} = KV(1 + |V|/V_0), \tag{6.11}$$

where V_0 is some velocity scale, was tried with little success.

The simplest remedy is to introduce a viscous boundary layer similar to Munk's (1950) wind-driven model by

$$\mathcal{D} = KV - \nu V_{xx}, \tag{6.12}$$

where ν is an eddy viscosity. This changes (6.6) to the fourth-order ODE

$$\nu L^2 T_{xxxx} - KL^2 T_{xx} - aT_x + \gamma T = \gamma T_L \tag{6.13}$$

to be solved with the extra no-slip condition

$$V = 0 \tag{6.14}$$

at the coasts. There are now four zonal length scales. Effectively one is still the long-wave scale D_E. The other three, D_W, d_E and d_W, are approximately $(\nu L^2/a)^{1/3}$. (Note the weaker dependence on a.) These shorter scales represent a simple easterly decay d_E matching V to 0 at the east coast, and an oscillatory decay d_W, D_W from the west. Writing

$$\begin{aligned} T = T_L &+ E_1 \exp[(x - x_E)/D_E] \\ &+ E_2 \exp[(x - x_E)/d_E] + \exp[-(x - x_W)/D_W] \\ &\times \{W_1 \cos[(x - x_W)/d_W] \\ &+ W_2 \sin[(x - x_W)/d_W]\}, \end{aligned} \tag{6.15}$$

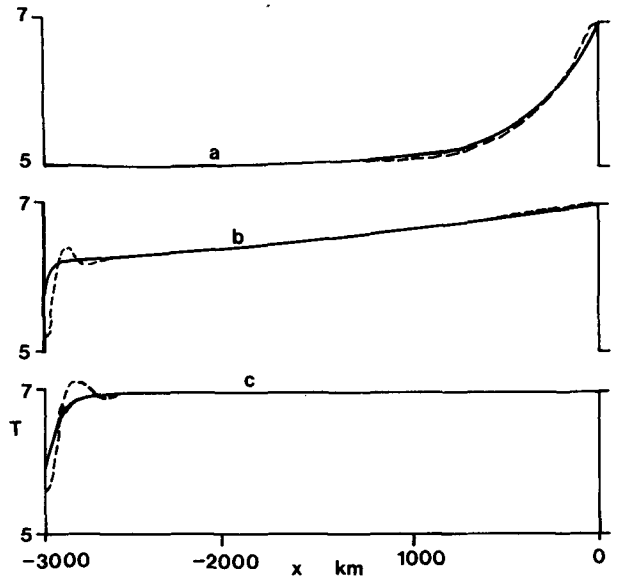

FIG. 14. Zonal sections of T_I for steady linear model with forcing as for Fig. 13. (a) y = 2000 km, (b) y = 1000 km, (c) y = 0 km for K = 0.1 day^{-1}, ν = 0 (solid, corresponds to Fig. 13), and for K = 0, $\nu = 2 \times 10^2$ m^3 s^{-1} = 170 km^2 day^{-1} (dashed, corresponds to Fig. 15).

we can find $E_1(y)$, etc., from the boundary conditions.

As an example, results with $\nu = 2 \times 10^3$ m^2 s^{-1} = 170 km^2 day^{-1} and K = 0 are given. (This choice for ν gives D_W, etc., about 50 km.) The map of T in Fig. 15a shows the usual eastern region, and a western boundary layer with characteristic current/countercurrent structure. This oscillatory behavior also appears in the vertical velocity map (Fig. 15b). The maximum poleward velocity is 0.34 m s^{-1}, with maximum countercurrent 0.05 m s^{-1}. Zonal T sections are given in Fig. 14. (Note how little the eastern region is changed.) When $K > 0$ is included, the western oscillations are damped.

There is virtually no countercurrent for K = 0.1 day^{-1}.

Most of the basin is controlled by long waves, and is little affected by the form of $\mathcal{D}$ because eastern longshore decay scales are very large.

b. *Nonlinear*

Combining (6.1) and (6.2) gives

$$\tfrac{1}{2}S\nabla\cdot\mathbf{U} - c_L A_1 T_x - A_2 U\cdot\nabla T - \tfrac{1}{2}A_3 U\cdot\nabla(\mathbf{U}\cdot\nabla T) + \gamma(T - T_L) = 0. \quad (6.16)$$

The term $\mathbf{U}\cdot\nabla(\mathbf{U}\cdot\nabla T)$ contains y derivatives, so this general nonlinear equation cannot be solved simply as an ODE with respect to x at a particular latitude. When $\mathcal{D}$ is linear in V, as in (6.12), we write

$$\mathbf{U}\cdot\nabla(\mathbf{U}\cdot\nabla T) = f^{-2}U\cdot\nabla(f^2\mathbf{U}\cdot\nabla T) - 2\beta f^{-1}V\mathbf{U}\cdot\nabla T.$$

The y derivatives only occur in the first term on the right, and are all of the form T_y. We expect nonlinear effects are important only near the coasts, where V is largest. But T_y is small in such regions due to the large longshore scale, so it seems reasonable to neglect this term. (Similar approximations can be used for quadratic or other terms in $\mathcal{D}$.)

The nonlinear model can then be conveniently solved numerically as follows. Starting from (x_E, y_S) where $T = T_L(y_S)$ is known, first solve the ODE assuming no west coast influence ($T \to T_L$ as $x \to -\infty$). Knowing $\mathcal{D}$ at x_E, step T up the coast using (6.4), solve at the new latitude, and repeat the process. Then add a west coast correction by similarly stepping down x_W from y_N, matching to the known eastern solution far from the coast. Note that with $\nu \neq 0$ we have $\mathbf{U} = 0$ at the coasts, so (6.16) reduces to a linear equation there allowing a good first guess. The calculation can be further simplified by using the long-wave approximation away from the boundary layers.

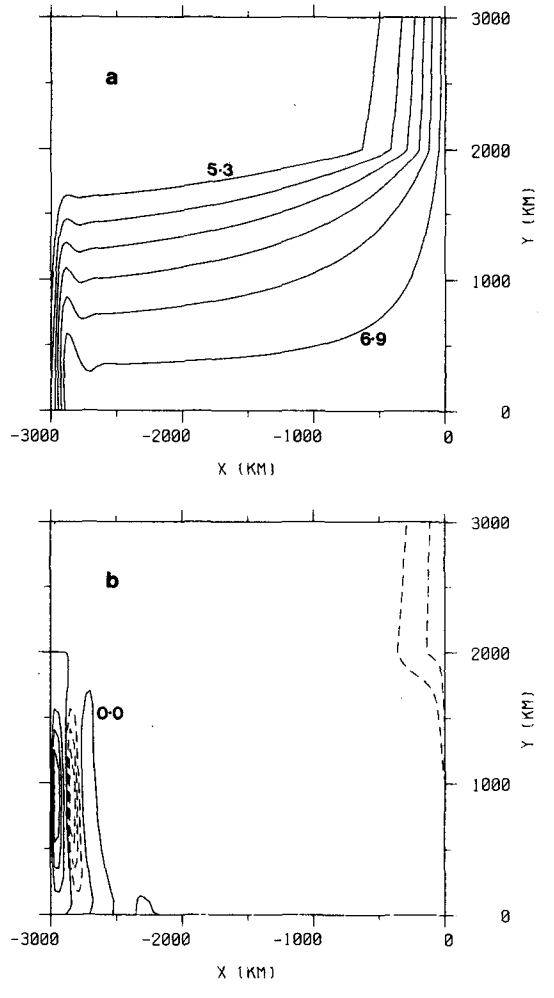

FIG. 15. As for Fig. 13, but with K = 0 and ν = 170 km^2 day^{-1}: (a) T_I = 5–7.2°C and (b) $w_I = -5.5 \times 10^{-11}$–$3.3 \times 10^{-10}$ m s^{-1}.

This also helps avoid numerical difficulties associated with $D_E \gg D_W$ etc.

The solutions obtained for T are quite like the linear results above. The main nonlinear effect is the change in S due to the term $\mathbf{U} \cdot \nabla T$, and this is only important near the coasts. Fig. 16 shows T_1 and T_2 for a nonlinear model with $K = 0.1$ day^{-1}, $\nu = 170$ km^2 day^{-1} and $T = (1 - \delta)\tau/\delta$. These maps are dominated by large perturbations (positive for T_1 and negative for T_2) near the west coast, where the static stability is still unreasonably large. Corresponding zonal sections of T are given in Fig. 17. Note that T still varies only slowly along the coasts, and that the western countercurrent is damped by $K > 0$. For a larger benthic timescale $\mathcal{T}$ the western boundary layer is thinner and S even larger there.

Though there are difficulties with the western boundary, this region has little effect on the rest of the ocean in this model, so the nonlinear model can be used to investigate the eastern region further. Static stability is smallest at the east coast, and one question of interest is whether reduced S allows T to vary more rapidly alongshore due to the associated decrease in offshore scale D_E and increased V and $\mathcal{D}$. Fig. 18 shows profiles of S and T along the east coast for $\nu = 0$ and $K = 0.1$ day^{-1}. Here atmospheric $T_N = 6$ (instead of the usual 8°C) and $T = 3(1 - \delta)\tau/\delta$ has been used. The offshore scale is large while $T_{Ay} < 0$, so V is small and nonlinear effects are negligible until y approaches 2000 km. Then V increases rapidly to about 0.12 m s^{-1} and the damping term KV^2 causes S to increase somewhat (reversing the decreasing trend to that point). Despite the relatively large V, however, T is still almost constant along the east coast. The local (no-coast) values S_L and T_L are included in Fig. 18 for comparison.

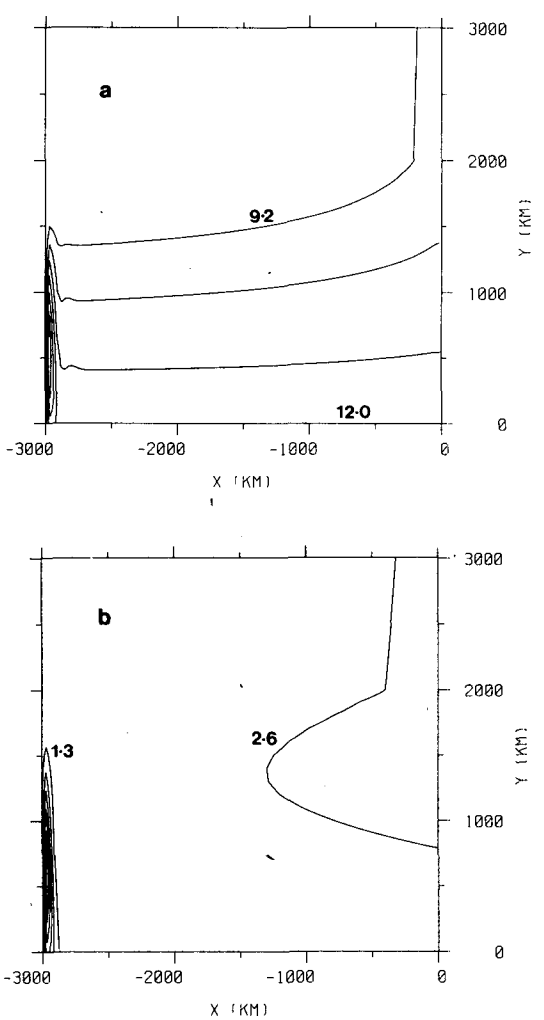

FIG. 16. Steady nonlinear model with east and west coasts, forcing as for Fig. 13, $K = 0.1$ day^{-1}, $\nu = 170$ km^2 day^{-1}: (a) $T_1 = 8.0$–16.5°C and (b) $T_2 = -5.1$–4.0°C.

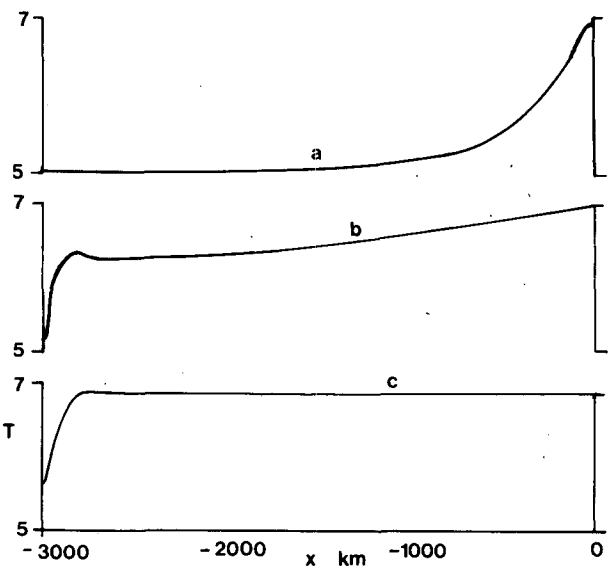

FIG. 17. Zonal sections of T_I corresponding to Fig. 14, at (a) $y = 2000$ km, (b) $y = 1000$ km, (c) $y = 0$ km.

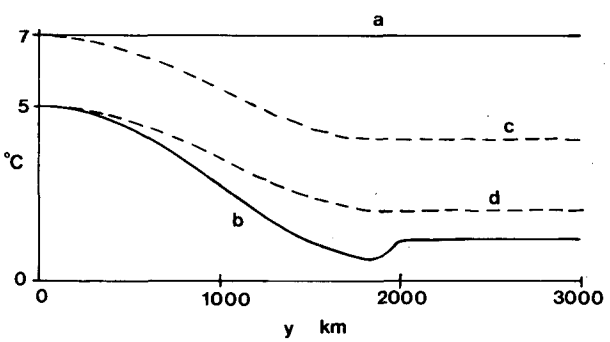

FIG. 18. Profiles along east coast for steady nonlinear model with $\delta T = 3(1 - \delta)\tau$, $T_A(y_n) = 6$°C, $\nu = 0$, $K = 0.1$ day^{-1}: (a) $T_I(x_E)$, (b) $S(x_E)$. The dashed curves are the local (no coast) profiles (c) T_L, (d) S_L.

7. Summary

An elementary two-level model with large-scale temperature forcing has been described. The aim is to explore some of the processes affecting the distribution of density while avoiding the complexities of numerical modeling. With temperature allowed to vary at each level effects such as dependence of surface heat flux on ocean temperature, the influence of density structure on wave speeds, and the generation of regions of weak static stability (potential deep-convection areas) can be investigated.

In response to a change in forcing there is first a rapid coastal response, followed by Rossby wave spinup on the much slower time scale τ (essentially an upper layer effect) extending a distance $c\tau$ from the eastern boundary. Finally there is a very slow change associated with benthic processes as a new steady state is approached.

For forcing that is colder poleward, the general upper level picture (qualitative at best) is of eastward zonal flow with poleward coastal currents (strongest near the western boundary). The lower level circulation is weaker and oppositely directed. There is weak downwelling over a relatively warm broad eastern region, associated with long Rossby waves that decay while travelling away from the east coast, and upwelling in the colder, narrower western boundary layer. This density pattern is similar to that observed in the North Atlantic during the 1962 *Erika Dan* cruise [see the atlas by Worthington and Wright (1970)]. In particular, the zonal section at 53°N shows warmer (and less dense) water over a broad eastern region. However, for a model with such simple forcing (and no wind stress) this evidence must be regarded as circumstantial.

The density changes near coasts are associated with Kelvin waves which tend to flatten longshore isopycnals. (Only the first baroclinic mode appears in the two-level model.) The longshore scale near the eastern boundary is very large (unless static stability is very small), and $T_I = \frac{1}{2}(T_1 + T_2)$ is almost constant there, even for rather large damping. Further investigation of this important feature is in progress.

There are a number of improvements and extensions that could be made. Inclusion of wind stress is straightforward, and potentially the most interesting addition because advection effects should increase. (With thermal forcing only, the advection terms are generally small due to the thermal wind balance. Further, stronger wind-driven currents are expected.) Seasonal variations can also be incorporated. For the resulting periodic solutions, a shorter longshore decay scale than that found for steady equilibrium is expected because ageostrophic effects are greater.

The most obvious deficiency is the primitive representation of forcing, and some form of surface mixed-layer model is needed if quantitative calculations are to be made. Better vertical resolution is desirable, particularly near the western boundary, though a variable thermocline depth may alleviate this problem. In a true basin model explicit benthic forcing by deep convection should be used. However, these modifications involve overturning and the ensuing complications lead back to numerical modelling.

Acknowledgments. Valuable advice from Dr. A. E. Gill and Dr. P. D. Killworth helped the development of this paper.

APPENDIX A

Derivation of Equations for Two-level Model

1. Continuous equations

The temperature equation in flux form is

$$T_t + \nabla\cdot(\mathbf{u}T) + (wT)_z = F, \tag{A1}$$

where F is a forcing term. In the absence of direct momentum forcing the linear equation for velocity $\mathbf{u}$ is, with the Boussinesq approximation,

$$\mathbf{u}_t + f\mathbf{k}\times\mathbf{u} = -\nabla p/\rho_c + \mathcal{D}(\mathbf{u}), \tag{A2}$$

where $\mathbf{k} = (0, 0, 1)$, p is pressure and $\mathcal{D}$ is a damping term. Small velocities are expected, so advection is omitted in the momentum balance. Nonlinear terms are retained in (A1), however, because changes in T may be relatively large. For hydrostatic conditions

$$p_z = -\rho g.$$

Density ρ is related to temperature by

$$\rho = \rho_c[1 - \alpha(T - T_c)]. \tag{A3}$$

Then (A2) and (A3) give

$$\mathbf{u}_{zt} + f\mathbf{k}\times\mathbf{u}_z = -\alpha g\nabla T + \mathcal{D}(\mathbf{u}_z). \tag{A4}$$

We have prognostic equations for $\mathbf{u}_z$ and T. Continuity provides a diagnostic equation for w:

$$w_z = -\nabla\cdot\mathbf{u}. \tag{A5}$$

With the bottom boundary at the constant depth $-H$ and a rigid lid at the surface $z_T = 0$, boundary conditions are

$$w_T = w_B = 0. \tag{A6}$$

The depth averaged velocity is

$$\bar{\mathbf{u}} = H^{-1}\int_{-H}^{0}\mathbf{u}dz.$$

When $\bar{\mathbf{u}}$ is initially zero, and there is no surface or bottom stress, we find $\bar{\mathbf{u}}$ is always zero. Then $\mathbf{u}$ is determined by $\mathbf{u}_z$ and the above set of equations is closed.

2. Two-level approximation

The temperature and continuity equations are applied at levels z_1 and z_2, and the velocity equation

(A4) is used at an intermediate level z_I. The vertical derivatives in (A1) and (A5) are approximated by, for example,

$$(Tw)_z(\mathbf{x}, z_1, t) \rightarrow (T_T w_T - T_I w_I)/(z_T - z_I).$$

Using (A5) and (A6) the temperature equations (A1) become

$$T_{jt} + \nabla \cdot (\mathbf{u}_j T_j) - T_I \nabla \cdot \mathbf{u}_j = F_j. \tag{A7}$$

Similarly we use

$$\mathbf{u}_z(\mathbf{x}, z_I, t) \rightarrow (\mathbf{u}_1 - \mathbf{u}_2)/(z_1 - z_2)$$

to write (A4) as

$$\mathbf{U}_t + f\mathbf{k} \times \mathbf{U} = -\nabla\phi + \mathcal{D}(\mathbf{U}), \tag{A8}$$

where

$$\left.\begin{aligned} \mathbf{U} &= \mathbf{u}_1 - \mathbf{u}_2 \\ \phi &= \tfrac{1}{2}H\alpha g(T_I - T_c) \end{aligned}\right\}.$$

Here T_c is a reference temperature. The geostrophic thermal wind $\mathbf{U}_g$ is

$$f\mathbf{k} \times \mathbf{U} = -\nabla\phi. \tag{A9}$$

In finite difference form vanishing $\bar{\mathbf{u}}$ gives

$$H_1\mathbf{u}_1 + H_2\mathbf{u}_2 = 0. \tag{A10}$$

To close this system we need to relate T_I to T_1 and T_2. A simple linear relation is

$$T_I = \omega T_1 + (1 - \omega)T_2, \tag{A11}$$

where $0 < \omega < 1$ is some constant.

It is useful to write prognostic equations in terms of T_I (which drives $\mathbf{U}$) and the difference

$$S = \tfrac{1}{2}(T_1 - T_2)$$

which is a measure of static stability. Using the expressions above, (A7) gives

$$T_{It} + (\omega - \delta)\mathbf{U} \cdot \nabla T_I + 2\omega(1 - \omega)\nabla \cdot (\mathbf{U}S) = \omega F_1 + (1 - \omega)F_2, \tag{A12a}$$

$$S_t + \tfrac{1}{2}\mathbf{U} \cdot \nabla T_I + (1 - \delta - \omega)\nabla \cdot (\mathbf{U}S) = \tfrac{1}{2}(F_1 - F_2). \tag{A12b}$$

In a region with solid and/or periodic boundaries these equations conserve the temperature average. By choosing

$$\omega = 1/2$$

the total temperature variance is also conserved, as in the continuous system. [See appendix B. Multilevel numerical ocean models often use this choice (Bryan, 1969).] Other choices for ω have different advantages. For example, $\omega = \delta$ or $\omega = (1 - \delta)$ leads to linear wave speeds with the same dependence on δ as found in two-layer models. Selection of small ω makes $\mathbf{U}$ less sensitive to changes in T_1. Wells (private communication) uses $\omega = \delta$ in a two-level equatorial model with wind and thermal driving, to obtain a reasonable balance of pressure gradient and wind stress.

3. Relation to shallow water equations

Two special cases are described, for which the model reduces to a form analogous to the shallow water equations with a mass source/sink.

a. Deep lower layer

When $H_2 \gg H_1$ the response to surface forcing is effectively confined to the upper level. In the limit $\delta \rightarrow 0$, we find $\mathbf{u}_2 \rightarrow 0$ and $\mathbf{u}_1 \rightarrow \mathbf{U}$. From (A8), finite HT_I is needed for finite $\mathbf{U}$. This can be achieved by choosing, for example, $\omega = \delta$, in which case $T_I \rightarrow T_2$ but $HT_I \rightarrow H_1T_1$ as $\delta \rightarrow 0$. Then from (A7)

$$T_{1t} + \nabla \cdot (\mathbf{U}T_1) = F_1, \tag{A13}$$

which with (A8) can be solved for T_1 and $\mathbf{U}$.

b. Linear model with $\mathcal{T} = \tau$

Consider $F_1 = (T_A - T_1)/\tau$ and $F_2 = (T_B - T_2)/\mathcal{T}$, as defined in Section 2, and suppose $\mathcal{T} = \tau$. Then (A12a), linearized about constant temperatures T_{10} and T_{20}, becomes

$$T_{It} + 2\omega(1 - \omega)S_0\nabla \cdot \mathbf{U} = (\omega T_A + (1 - \omega)T_B)/\tau - T_I/\tau. \tag{A14}$$

Eqs. (A8) and (A14) form a closed system for $\mathbf{U}$ and T_I. We also find

$$(H_1T_1 - H_2T_2)_t + (H_1T_1 - H_2T_2)/\tau = (H_1T_A - H_2T_B)/\tau; \tag{A15}$$

thus $H_1T_1 - H_2T_2$ can be found independently, and hence T_1 and T_2 obtained. (See also Section 5.6 for the corresponding nonlinear geostrophic case.)

APPENDIX B

Conservation Properties

We let angle braces denote the average over a horizontal area with fixed impermeable and/or periodic boundaries, and denote the finite-difference form of the vertical average by an overbar. From (A7) and (A10) we find

$$\langle T_1 \rangle_t = \langle T_I \nabla \cdot \mathbf{u}_1 \rangle + \langle F_1 \rangle = -(1 - \delta)\langle \mathbf{U} \cdot \nabla T_I \rangle + \langle F_1 \rangle, \tag{B1}$$

and similarly

$$\langle T_2 \rangle_t = \delta \langle \mathbf{U} \cdot \nabla T_I \rangle + \langle F_2 \rangle. \tag{B2}$$

Hence the time variation of average temperature is

$$\overline{\langle T \rangle}_t = \overline{\langle F \rangle}, \tag{B3}$$

so $\overline{\langle T \rangle}$ is conserved in this volume when there is no forcing.

From (A7) we also have

$$\tfrac{1}{2}\overline{\langle T^2 \rangle}_t + \overline{\langle T\nabla\cdot(\mathbf{u}T)\rangle} - \overline{\langle T_I\nabla\cdot\mathbf{U}\rangle} = \overline{\langle TF\rangle},$$

which can be rearranged using (A10) to give

$$\tfrac{1}{2}\overline{\langle T^2 \rangle}_t + \tfrac{1}{2}\delta(1-\delta)\overline{\langle (T_1 - T_2)} \times (T_1 + T_2 - 2T_I)\nabla\cdot\mathbf{U}\rangle = \overline{\langle TF\rangle}. \quad \text{(B4)}$$

For the choice

$$T_I = \tfrac{1}{2}(T_1 + T_2),$$

we have

$$\tfrac{1}{2}\overline{\langle T^2 \rangle}_t = \overline{\langle TF\rangle}, \quad \text{(B5)}$$

and temperature variance is conserved in the absence of forcing. Note that these conservation properties do not depend on the momentum equations.

Through the velocity equations the term $\langle \mathbf{U}\cdot\nabla T_I\rangle$ is related to the rate of change of kinetic energy, the form of the kinetic energy depending on the actual equations [see (2.17a), for example]. Energy conservation can then be derived from (B1) and (B2).

When $T_I = \tfrac{1}{2}(T_1 + T_2)$, we can also obtain from (A7)

$$(H_1T_1 - H_2T_2)_t + 2H\delta(1-\delta)\mathbf{U}\cdot\nabla T_I = (H_1F_1 - H_2F_2), \quad \text{(B6)}$$

and hence find a Bernoulli function. For example, (2.17a) leads to

$$[\alpha g(H_1T_1 - H_2T_2) - 2\delta(1-\delta)V^2]_t = \alpha g(H_1F_1 - H_2F_2) + 4\delta(1-\delta)V\mathcal{D}; \quad \text{(B7)}$$

thus the term in brackets is conserved in the absence of damping and forcing.

APPENDIX C

An Unstable Free Mode for the Frozen f Model

The velocity equations (2.14), with $\mathcal{D} = 0$, can be written

$$f_0V = \phi^*_x, \quad \text{(C1a)}$$

$$ff_0U = -\beta\phi^* - f\phi^*_y - \phi^*_{xt}, \quad \text{(C2)}$$

where

$$f\phi^* = f_0\phi.$$

The divergence is

$$\nabla\cdot\mathbf{U} = -(\beta\phi^*_x + \phi^*_{xxt})/ff_0,$$

so the linearized equation (2.20) becomes (omitting F for convenience)

$$(f/f_0)^2\phi^*_t - L_0^2(\beta\phi^*_x + \phi^*_{xxt}) = 0 \quad \text{(C3)}$$

where $L_0^2 = g'H/f_0^2$.

A constant f in (C2) and (C3) gives the consistent equations

$$f_0^2U = -\beta\phi^* - f_0\phi^*_y - \phi^*_{xt}, \quad \text{(C1b)}$$

$$\phi^*_t - L_0^2(\beta\phi^*_x + \phi^*_{xxt}) = 0. \quad \text{(C4)}$$

Vanishing U at east and west coasts requires

$$\phi^*_{xt} + \beta\phi^* + f_0\phi^*_y = 0 \quad \text{(C5)}$$

at x_E and x_W. Sinusoidal meridional modes can now be used to conveniently solve for ϕ^* by separating the y and x, t dependence.

The solution

$$\phi^* = X(x)\exp(ily + \sigma t)$$

requires, from (C4),

$$\sigma X - L_0^2(\beta X_x + \sigma X_{xx}) = 0. \quad \text{(C6)}$$

There is a mode with $\mathbf{U} \equiv 0$ that automatically satisfies (C5). This requires

$$\sigma X_x + (\beta + ilf_0)X = 0, \quad \text{(C7)}$$

which has a solution

$$X = \exp(\Lambda x),$$

where

$$\Lambda = -(\beta + ilf_0)/\sigma.$$

Combining this with (C6) we can find σ with $\mathrm{Re}(\sigma) > 0$, which represents a mode growing in time (and spatially decaying eastward). Veronis (1966) mentions a similar Rossby wave instability when f is constant.

Physically the instability can be explained by considering an energy equation. From (C1) and (C4) we have

$$[\phi^{*2} + (L\phi^*_x)^2]_t = \beta L^2(\phi^{*2})_x + 2L^2(\phi^*\phi^*_{xt})_x = -\beta L^2(\phi^{*2})_x - 2g'H\nabla\cdot(\mathbf{U}\phi^*). \quad \text{(C8)}$$

Integrating over a north–south periodic area between the coasts gives

$$\langle \phi^{*2} + (L\phi^*_x)^2\rangle_t = \beta L^2\int \phi^{*2}(x_W) - \phi^{*2}(x_E)dy. \quad \text{(C9)}$$

The right-hand side is positive for a west coast Kelvin wave, which has amplitude decaying eastward. [The right-hand side vanishes for the variable version of (C8).]

Interestingly, the term in angle braces is conserved if

$$\tfrac{1}{2}\beta\phi^* + f_0\phi^*_y + \phi^*_{xt}$$

vanishes at x_E and x_W. Unfortunately it does not seem possible to find a conservative separable model with consistent equations and boundary conditions for a mid-latitude β-plane.

APPENDIX D

Nonlinear Long Waves

For the nonlinear long waves in Section 5 (with $\mathcal{T} = \tau$), we found

$$T_t - c(1 + S'/S_0)T_x - \delta U_L T_x = F, \quad \text{(D1)}$$

$$S' = (1 - 2\delta)(T - T_L) + \tfrac{1}{2}\Delta[1 - \exp(-t/\tau)]. \quad \text{(D2)}$$

Eq. (D1) can be written as an equation for $T - T_L$, i.e.,

$$(T - T_L)_t - c[1 + S'/S_0 + \delta U_L](T - T_L)_x + (T - T_L)/\tau = 0. \quad \text{(D3)}$$

Then by defining a new dimensionless variable h by

$$T - T_L = \tfrac{1}{2}\Delta h \exp(-t/\tau) \quad \text{(D4)}$$

and substituting for S' using (D2), we have

$$h_t - c\{1 + \mu[1 - \exp(-t/\tau)] + \eta h \exp(-t/\tau)\}h_x = 0, \quad \text{(D5)}$$

where

$$\left.\begin{aligned} \eta &= (1 - 2\delta)\Delta/2S_0 \\ \mu &= (\Delta - 2\delta T_{Ay} f/\beta)/2S_0 \end{aligned}\right\}.$$

Boundary conditions for (D5) are

$$h = \begin{cases} 0, & \text{at} \quad t = 0, \quad \text{(D6a)} \\ \exp(t/\tau) - 1, & \text{at} \quad x = x_E. \quad \text{(D6b)} \end{cases}$$

At a given latitude, μ and η are constant, so (D5) can be solved as an x, t problem using characteristics. The term h is constant along a characteristic, and this information travels at speed $dx/dt = -c\{\ \}$. From position (x_E, t_0) these characteristics carry

$$h = \left\{\begin{matrix} \exp(t_0/\tau) - 1, & t_0 \geq 0 \\ 0, & t_0 \leq 0 \end{matrix}\right\} \quad \text{(D7)}$$

to the position

$$x = x_E - c\{(1 + \mu)(t - t_0) - \tau[\eta + (\mu - \eta) \times \exp(-t_0/\tau)][1 - \exp(-(t - t_0)/\tau)]\} \quad \text{(D8)}$$

at time t. Given x and t, (D8) can be easily solved to find t_0, and hence find h, then T. The position of the wavefront can be found explicitly. It leaves x_E at $t = 0$ to travel to

$$x = x_E - c\{(1 + \mu)t - \mu\tau[1 - \exp(-t/\tau)]\} \quad \text{(D9)}$$

at time t.

REFERENCES

Adamec, D., R. L. Elsberry, R. W. Garwood and R. L. Haney, 1981: An embedded mixed-layer ocean circulation model. *Dyn. Atmos. Oceans*, **6**, 69–96.

Anderson, D. L. T., and A. E. Gill, 1975: Spin-up of a stratified ocean, with applications to upwelling. *Deep Sea Res.*, **22**, 583–596.

——, and P. D. Killworth, 1979: Nonlinear propagation of long Rossby waves. *Deep Sea Res.*, **26A**, 1033–1050.

Barcilon, V., 1971: A simple model of the thermocline in a bounded ocean. *J. Phys. Oceanogr.*, **1**, 7–11.

Bryan, K., 1969: A numerical method for the study of the circulation of the world ocean. *J. Comput. Phys.*, **4**, 347–376.

——, and M. D. Cox, 1967: A numerical investigation of the oceanic general circulation. *Tellus*, **19**, 54–80.

Fofonoff, N. P., 1962: Dynamics of ocean currents. *The Sea*, M. Hill, Ed., Vol. 1, Interscience, 323–395.

Haney, R. L., 1971: Surface thermal boundary conditions for ocean circulation models. *J. Phys. Oceanogr.*, **1**, 241–248.

Killworth, P. D., 1974: A baroclinic model of motions on Antarctic continental shelves. *Deep Sea Res.*, **21**, 815–837.

Lighthill, M. J., 1969: Dynamic response of the Indian Ocean to onset of the Southwest Monsoon. *Phil. Trans. Roy. Soc. London*, **A265**, 45–92.

Lorenz, E. N., 1960: Energy and numerical weather prediction. *Tellus* **12**, 364–373.

McCreary, J., 1976: Eastern tropical ocean responses to changing wind systems: with applications to El Niño. *J. Phys. Oceanogr.*, **6**, 632–645.

Munk, W. R., 1950: On the wind-driven ocean circulation. *J. Meteor.*, **7**, 79–93.

Robinson, A. R., and P. Welander, 1963: Thermal circulation on a rotating sphere; with application to the oceanic thermocline. *J. Mar. Res.*, **21**, 25–38.

Sarmiento, J. L., and K. Bryan, 1982: An ocean transport model for the North Atlantic. *J. Geophys. Res.*, **87**, 394–408.

Stommel, H. M., 1948: The westward intensification of wind-driven ocean currents. *Trans. Amer. Geophys. Union*, **29**, 202–206.

Veronis, G., 1966: Rossby waves with bottom topography. *Deep Sea Res.*, **24**, 338–349.

——, 1973: Model of world ocean circulation. I. Wind-driven, two layer. *J. Mar. Res.*, **31**, 228–288.

——, 1976: Model of world ocean circulation. II. Thermally driven, two layer. *J. Mar. Res.*, **34**, 199–216.

Welander, P., 1971: The thermocline problem. *Phil. Trans. Roy. Soc. London*, **A270**, 415–421.

White, W., and R. Bernstein, 1981: Large-scale vertical eddy diffusion in the main pycnocline of the central North Pacific. *J. Phys. Oceanogr.*, **11**, 434–441.

Worthington, L. V., and W. R. Wright, 1970: *North Atlantic Ocean Atlas. WHOI Atlas Series*, Vol. 2.